

Anonymous Referee #1

Received and published: 21 October 2019

The authors analyzed a unique data set on year-round particle size distribution (PSD) measured at the coastal Antarctic station Halley. They based their data evaluation on statistical cluster analysis, which has been applied as beneficial tool in several comparable investigations (References: Dall'Osto et al., 2019, 2018, and 2017). The manuscript at hand presents valuable, meaningful, and novel findings from a region where only very few studies on the variability of aerosol physical properties are available.

Many thanks for appreciating the manuscript.

Without doubt, the topic addresses the scientific scope of ACP, particularly considering the fact that aerosol-cloud interaction in the southern Ocean realm is still poorly understood leading to strong biases in climate modelling. Most notably in this context, PSD measurements from this region are qualified for assessing the potential of the aerosol to act as cloud condensation nuclei (CCN). Hence, I recommend a final publication after some more or less basic revisions.

Many thanks again for appreciating the manuscript.

General issues:

(i) Presentation and discussion of the results are largely restricted to the "higher-level" output of the cluster calculations. Therefore, you should clearly substantiate the advantages and benefits of this method. The short section provided on page 6, lines 1 to 8 appears scarce. To be more specific (or even provocative): Two of the main conclusions drawn from this study and mentioned in the Abstract as point (1) and (2) (page 2, lines 22 to 28) can be easily derived without using any cluster analysis.

The cluster analysis has been proven successful in many previous studies (cited in the manuscript, Dall'Osto et al. 2010-2018 and Beddows et al., 2009-2016) where the advantages and benefits were shown. In a nutshell the clustering analysis can greatly simplify the interpretation of aerosol size distributions. Indeed we show in page 6 line 8-20 two examples. Nevertheless, we briefly expanded the section and references.

(ii) Moreover, from my point of view, it would be beneficial or even necessary to focus from case to case more on the original SMPS data, primarily when assigning air mass origins to NPF events. Here a more detailed discussion of air mass histories along with the original, individual PSD-spectra could be much more meaningful (the sketchily approach presented on page 14, lines 12 to 32 is hardly adequate).

We expanded this section and added a NPF formation events and described it (see Figure SI9) and text in the section.

In case of “Nucleation” cluster: Do the individual PSD-spectra show particle growth in contrast to the spectra assigned to “Bursting”? Especially here, you may present some examples from the original data set to demonstrate the unique characteristic.

This paper has already 8 main Figures and 9 Supporting information Figures. We added into words two typical PSD-spectra (already described in many previous papers - Dall'Osto et al., 2017, 2018, 2019 and we feel we do not need to repeat them again). We added an example of a nucleation cluster episode (Figure SI9) and described in words that "bursting" are not defined events where grown is not seen (often also called "apple events").

(iii) Air mass back trajectory analysis is a fundamental scaffolding of this study. The trajectory cluster analysis is interesting on its own but, however, somewhat detached from the PSD cluster analysis. I recommend presenting a figure analogous to Fig. SI 7 in the main text, but showing here trajectory ensembles sorted according to the PSD clusters as described on page 14, lines 12 to 32. Just another (minor) point concerning Fig. SI 7: The plot for cluster 1 (sea ice) shows terrain heights typically around 200 m or so, though the air masses travelled across the Weddell Sea (terrain height should be around zero!) – please check and clarify!

The calculation leading to the plot of C1 in Fig SI7 is correct. The aggregated back trajectory starts at a height of 692m above the ground (terrain) and arrives at 10m above the receptor site. We can't lower this without the trajectories grounding. But the average trajectory does not reflect the wide spread of height values. The median trajectory height is around 300m with a lower 25th quartile has heights between 5 and 10. This is further exemplified by a comparison between the histogram of step heights of the trajectories for cluster 1 and nominally cluster 6. It is clear from these that histogram of heights is heavily skewed towards low-level trajectories.

(iv) I recommend moving Figures SI 3 and SI 4 presented in the Supplementary Information (SI) to the main text, because they contain crucial information.

We considered it, however Figure SI4 is basically a repetition of Figure SI2, and given we already have 8 main Figures in the manuscript, and we added to additional SI Figures (now 9 in total) we decided to leave them in SI material.

(v) Whenever possible, provide corresponding uncertainties or standard deviations of the results, especially for any values given in “%” (regarding text and figures).

Given average errors in legends, about 25% average.

(vi) The pivotal question you raise addresses the balance between secondary vs. primary aerosol in this region (see Abstract lines 8 to 11 and p. 16, lines 2 to 4). I suggest picking up this quest in your conclusions more explicitly.

We edited it and expand briefly the conclusions.

Finally: Do you have any suggestion for future research on this topic?

We edited and explained that further studies will analyze the SMPS data from multiple stations for the year 2015.

Some specific and minor points:

1. Abstract: Please concretely state here size range, temporal resolution and measuring period.

Edit. 6-209 nm in size range, daily resolution

2. Page 4, line 29: . . .higher NPF instead of higher N.

Edited

3. Chapter 3.2: The association of PSD with meteorology, physical and chemical parameters appears rather descriptive. Do you have any ideas regarding the physical background of your findings?

We expanded this section

4. Page 9, lines 17 to 19: Hijman (2019) and Becker (2018) are not listed in the references.

Edited and modified

5. Page 14, line 19: Why did you relate to a total travel time of just 60 h and not 120 h (5 days back trajectories)?

Based on previous studies (Dall'Osto et al., 2017, 2018) we chose to focus on shorter air mass trajectories to study new particle formation and bursting aerosol categories.

6. Page 16, line 12: Please state "low particle number concentrations" more precisely.

Edited, 121-279 particles cm-3

7. Page 17, lines 5 to 16: I guess, during winter nss-sulphate aerosol should be negligible compared to sea salt. Maybe an additional closer look into the material presented in Rankin and Wolff (2003) or previous results on the chemical composition of the bulk aerosol from that site could be revealing, especially assessing the role of primary aerosol acting as CCN.

We edited the text. However, it should be kept in mind that aerosol mass and aerosol number concentrations can be misleading - comparing PM mass with aerosol number concentrations may lead to wrong conclusions.

8. Page 18, line 16: Please state “baseline” more precisely.

Edited, annual average

9. Figure 4, caption, line 9: . . . during the year 2015 (not: during the year 365).

Edited

Interactive comment on “On the annual variability of Antarctic aerosol size distributions at Halley research station” by Thomas Lachlan-Cope et al.

Anonymous Referee #2

Received and published: 6 November 2019

The authors analyze particle size distribution data from coastal Antarctica using statistical methods to draw conclusions about aerosol sources and atmospheric processes. The results presented are both valuable and novel and are definitely within the scope of ACP. The context of the analysis and some of the actual discussion, especially as it relates to the existing literature, needs to be expanded but the necessary additions are minor with regards to the overall manuscript. Therefore, I recommend final publication with (generally) minor revisions.

Many thanks for the appreciation of the paper

Major comments:

Clustering analysis (especially S.2.2.1 and S.3.1.2) – The discussion on the clustering analysis needs to be greatly expanded as this is a fairly novel technique in atmospheric science. Many people fall into the trap of thinking that this machine learning method is actually machine intelligence and simply gives a “correct” answer as opposed to a mathematically valid solution. First, the values given for the Dunn Index and Silhouette Width need to be given context. Primarily, plots of both versus cluster number should be offered as many readers have no experience using or analyzing cluster analysis results. Secondly, the values themselves need to be discussed in much greater detail. The 4x increase of the Dunn Index is good but 10^{-3} is still an extremely small value and implies that the clusters are extremely sparse (not compact), are not very far apart, or both. A graph of the cluster points to visually inspect both compactness and distance between clusters may be useful but may also be misleading as ambient data sets are often quite messy. Second, some additional validation of the cluster choice must also be presented.

We edited all new section 2.2.1 and added two additional SI Figures (SI 1 and SI2).

We agree with the Referee 2 in that there is a potential trap to fall into, thinking that this machine learning method is actually machine intelligence and simply gives a “correct” answer as opposed to a mathematically valid solution. This is why we only use cluster metrics as a rough guide to inform our decisions. More often than not, our approach is to use a higher number of clusters and then manually aggregate them according to their shape and temporal trends. This in itself ensure that we do not miss any details and helps us select the optimum setting for the analysis to produce a result which

best describes the environmental conditions. Consequently, we do not give so much value to the cluster statistics that they drive the analysis towards a mathematically valid solution over a valid environmental solution. Hence, below we have given a description of the metric we have used and agree that we can put these into context.

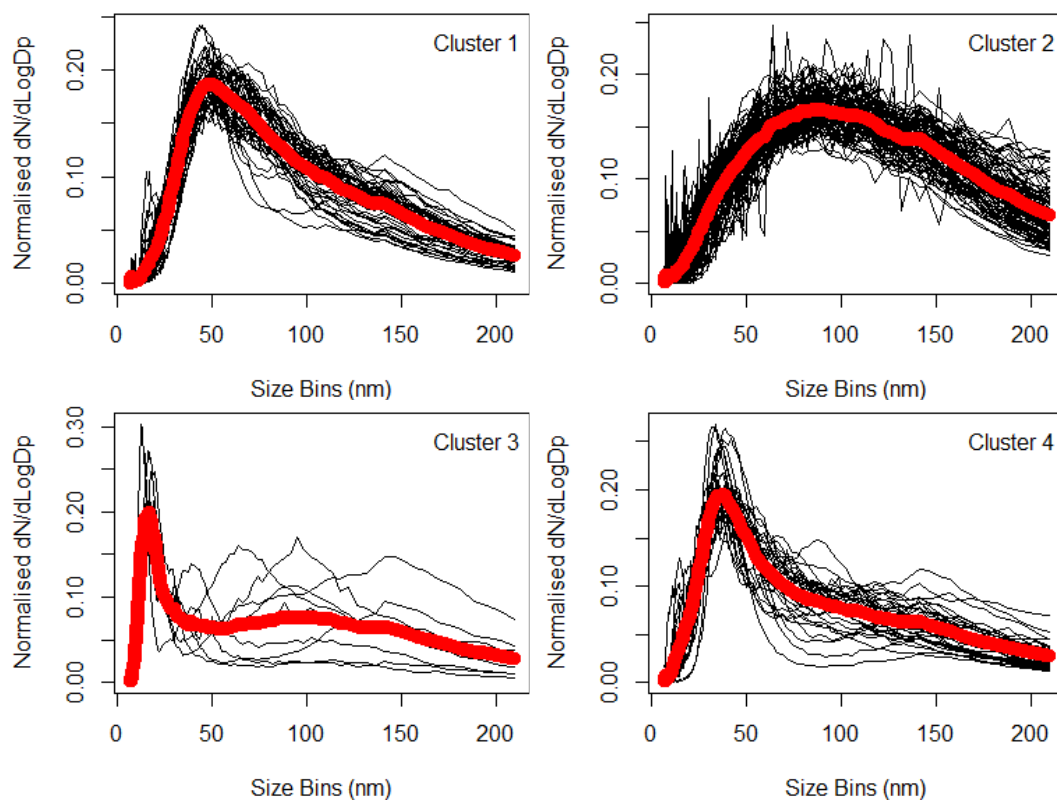
With this in mind, the validation Indices used in this study were the Dunn Index (DI) and the Silhouette Width (SW) and the reader is referred to two very useful papers in order to understand these metrics fully (Halkidi et al 2001 and Rousseeuw 1987). The DI value at its most simplest can be thought of as the ratio of the minimum Euclidian distance between any two elements in two different clusters d_{min} to the largest separation of two elements within any of the clusters d_{max} . A DI value of 1 is obtained for a dataset with $d_{max} = d_{min}$, i.e. where the largest diameter of a cluster is equal to the minimum separation of between the circumference of any two of the clusters. Similarly, a DI value of 0 is obtained when $d_{min} \ll d_{max}$, i.e. if the clusters are touching each other. On this scale, our values of the order of 10-3 are indicative of clusters which are close to touching each other. This is not helped by the normalisation of the NSD which removes the total magnitude of the particles count from the data but it is important that we NSD shape without any bias due to the number concentration in the NSD. We also need to remember that this DI reflects the proximity of the two most similar clusters and does not reflect the separation of the other clusters which will be larger. In fact, this minimum separation is susceptible to outliers in the clusters.

The Silhouette Width is a measure of how well the elements i of a cluster matches the cluster (i.e. how well it has been classified) and a good description of this metric can be found in Halkidi et al 2001. A value close to 1 indicates that the elements are classified correctly and a value of 0 indicates that the elements ought to be classified in a different cluster arrangement. Our value of around 0.4 (comparable to those discussed in Halkidi et al 2001) is the average value of the Silhouette Widths for all 8 clusters which ranges from 0.3 to 0.55. But to appreciate the quality of the clustering associated with the DI and SW values, Figure A presents the plots of the NSD for each cluster. Rather than a plot of points in an arbitrary space, we have used this to demonstrate the compactness and distance of the clusters. Each graph plots all of the daily average NSD for that cluster as a black curve and are compared with the average NSD plot of that cluster. From this figure, it is clear that we have good separation of the data for all of the clusters with the odd spurious NSD in clusters 1, 3, 4 and 7 which are not sufficient in number to form their own cluster but are allocated to their nearest cluster. It is these few sporadic NSD which lower the SW and DI values. From this optimum situation, it can be envisioned that as we reduce the number of clusters we will lose the integrity of the separation and we might well expect the cluster elements to aggregate into larger clusters according to their modal diameter, eg Clusters 1, 3, 4 and 7; clusters 2, 6 & 8; and cluster 6. In fact, when we calculate the minimum standard deviation of the points about the mean NSD for each cluster setting, this is a minimum for 8 clusters.

We can illustrate this further when we plot the cluster number (as a colour) against the first 2 principle components (PC1 and PC2) in a bivariate plot. From this, we can see the grouping of the clusters (Figure B). This plot shows that there is no clear separation between neighbouring clusters and hence it

follows that the DI is more sensitive to the compactness of the cluster and when used with the SW find the optimum grouping of the NSD. The Nascent and Aiken (1 and 4) clusters group together on the bottom of the plot. Clusters 3 and 7 are on the top right hand of the plot and describe the Nucleation and Bursting and define to separate areas of the plot. The remaining 3 clusters, named Pristine (2, 5 and 6) fill in the gap between these two groups of cluster in the PC1-PC2 space. The remaining cluster called Bimodal forms the boundary between the two Pristine clusters 2 and 6. How this PC1-PC2 space is divided up as we increase the number of clusters from 2 to 8 can also be visualised in Figure C. At 2 clusters, the space is divided about a vertical line at just less than PC1-0.0 and as we increase this to 4, the data can convincingly be seen to divide into 4 equal spaces. As we increase from 4 clusters, we start to separate out the more interesting details in the NSD data at 8 clusters where we start to separate out types of nucleation and bimodal distributions.

We think this is sufficient to give confidence that our method has produce convincing results and we refrain from extending the study as recommended in the second half of the 'Major Comments:.' to work on heavily curated data, leaving this to the possibility of a follow on methodology paper which is beyond the scope of this study. In fact, we are less inclined to include this under the bonnet/hood material discussed here in regards to figures A, B and C and use this in such a publication.



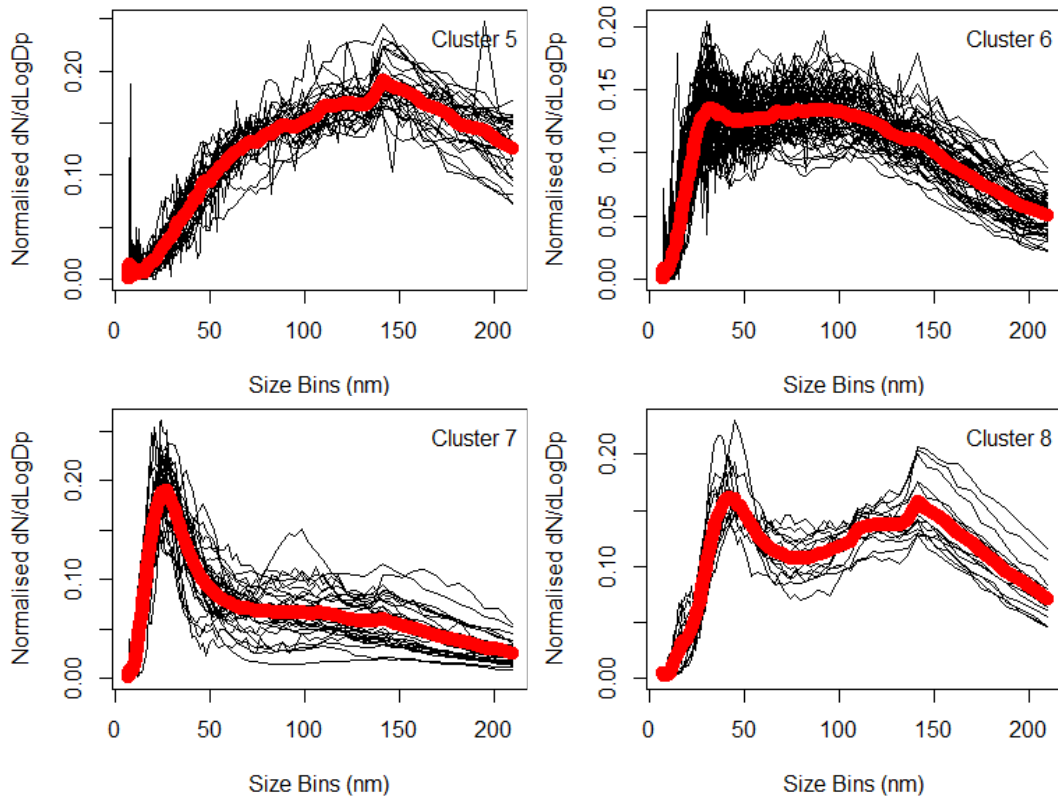


Figure A. Daily normalised number size distributions plotted for each cluster (black lines) and overlaid by the mean number size distribution for the cluster.

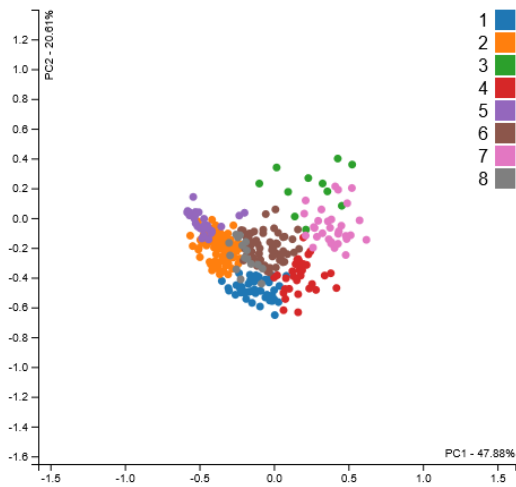


Figure B. Bivariate plot showing the 8 clusters plotted as a colour against the first 2 principle components PC1 and PC2.

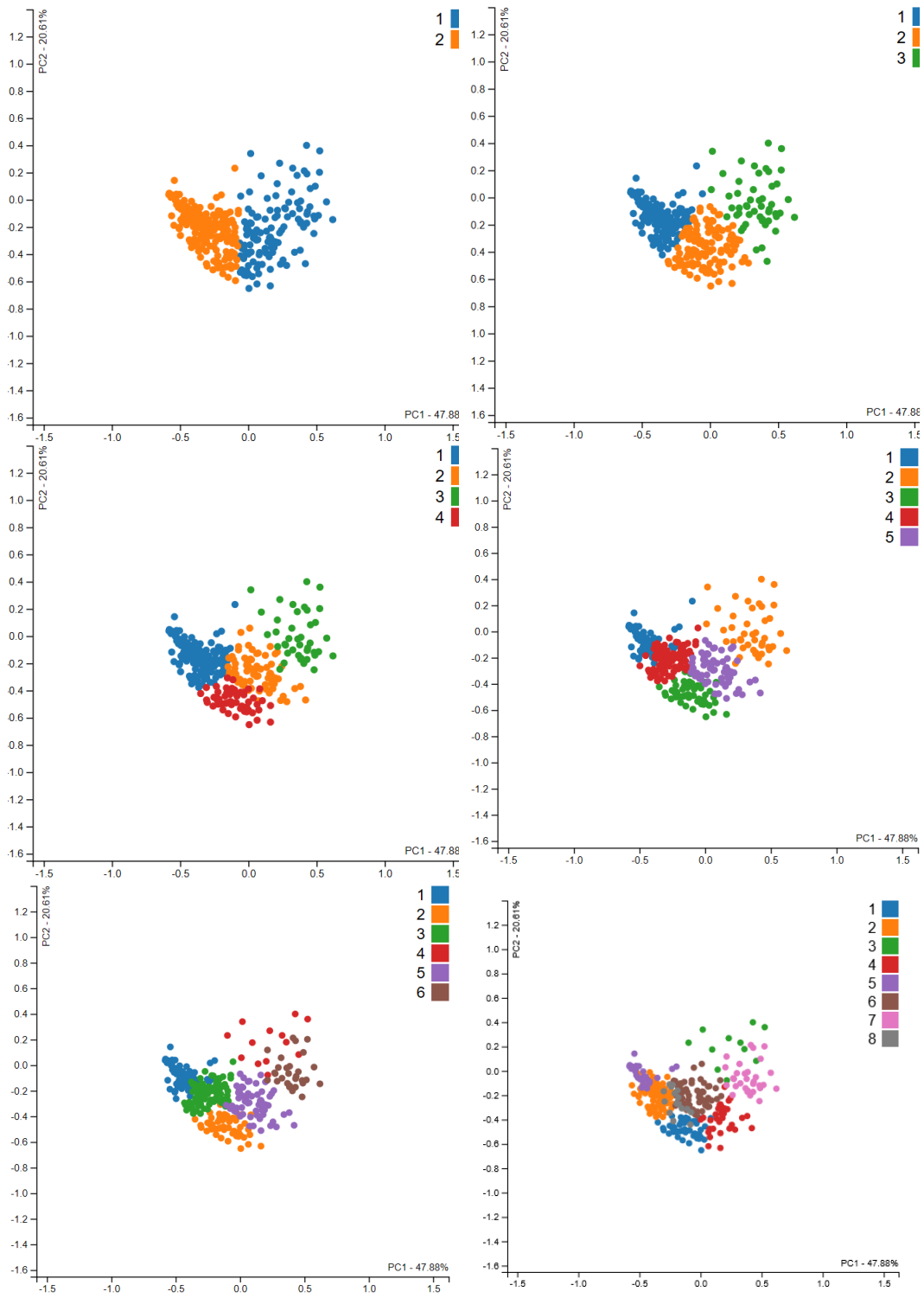


Figure C. Bivariate plots showing the clusters plotted as a colour against the

first 2 principle components PC1 and PC2. This figure shows how the NSD are clustered as the number of clusters is increased from 2 to 8 clusters.

One way to do this may be to perform the analysis on heavily curated data to see if the results broadly match the overall analysis. I would highly (and very strongly) recommend that the authors run the analysis on a time frame where there are a minimum number of clusters expected (e.g. June). If there is broad agreement between the results there and the overall results, this would lend a great amount of strength to the overall conclusions. This could, and possibly should, be done in the context of air mass back trajectories as well where air masses could be broadly classified relative to their time spent over the continent, sea ice, or open ocean (this also comes with major caveats though, also see minor comment about back trajectory analysis).

We addressed this above

S.2.3 – is missing?

Added

S.4.1 – Much of the length of this section could be moved into the introduction and the remaining text expanded to give a more complete view of how these results fit into the existing literature. Overall, the authors do a fine job of finding relevant papers but do not necessarily discuss the conclusions presented completely. In particular, more discussion regarding measured composition and size distributions and the results presented here may be useful.

The results of Rankin and Wolff (2003), Preunkert et al. (2007, 2008), Saiz-Lopez et al. (2007), Schmale et al. (2013), Giordano et al. (2017), and many others should likely be discussed in greater detail. Additionally, the presence and lack of photochemistry should be given some context as this is a fairly dominating factor in the polar regions' winter vs. summer months.

We tried to cite all the relevant papers, making sure the particulate matter mass and aerosol number concentrations could overlap. We edited all the papers and improved the text where possible. The majority of the studies report primary and secondary components in term of mass, which should not be confused with particle number concentration.

Diurnal profiles (Fig. SI 3 especially) – The basis of this analysis, especially considering the weight the figure is given in the text itself, needs to be better justified. Diurnal profiles are generally helpful in visualizing the impacts of either photochemistry or timed anthropogenic activities (or both). Neither of these cases apply to the Antarctic continent. Either the analysis should be rerun in a more nuanced approach (e.g. diurnals for periods of 24-hours of sunlight and lack thereof, only run in the short timeframes of clearly demarcated sunrise/sunset) and discussed in that context or should be

removed completely. These results could be analyzed to give important insights into the potential role that the Polar sunrise/sunset plays in aerosol size distributions but this analysis may be beyond the scope of this manuscript.

We do not have solar radiation data for this study. The impact of photochemistry may also be not straight forward as summer lacks of strong diurnal profiles. We agree this analysis is beyond the scope of this manuscript (already quite large given the 22 Figures presented).

Minor comments:

P.7, S2.2 – A few sentences about the transmission efficiency of the aerosol stack for relevant sizes of aerosols should be added. The authors could consider applying a correction to the size distributions to account for inlet losses but I imagine they are fairly small for the relevant sizes.

Indeed, as discussed in Jones et al., 2008 and in the text of this manuscript.

S.2.4 and 3.3 – A few sentences regarding the accuracy of HYSPLIT being used in regions of sparse meteorological measurements should be added. A more detailed description of the initialization conditions for the model should also be added.

Back trajectories calculations are not renowned as being accurate, especially the further away in time and space from the receptor site. Fleming et al Atmospheric Research 104-105 (2012) 1–39 give a brief overview in their introduction. But we might well see a further reduction in predictive capability of the back trajectories if the meteorological measurements are sparse.

Boccaro et al 2008 consider this problem for lower stratosphere over Antarctica. <https://doi.org/10.1029/2008JD010116>. Simulated trajectories were computed starting from the positions of the balloon and advected using the ECMWF velocity fields. The simulated trajectories are compared to the real balloon trajectories. The spherical distance between the real and simulated positions exceeds 1000 ± 700 km on average after 10 days using ECMWF. We use 5 day trajectories but can use this to help us gauge the accuracy at 5 days to be approximately 500 km which is just over the width of figure 4a. Clustered trajectories 1 is distinct from 2-6 due to its sole origin West of Halley. Whereas, the starting points of clustered trajectories 2-6 are all within this 500km uncertainty. Clearly, as the trajectory arrives at Halley, the uncertainty reduces to a minimum so we can have a higher confidence of the shape of the trajectories as they approach the receptor cite. With regards to the initialisation conditions: The meteorology files used are from the NCEP/NCAR Reanalysis Project is a joint project between the National Centers for Environmental Prediction (NCEP, formerly "NMC") and the National Center for Atmospheric Research (NCAR). The trajectories were collected with 10m, 30 and 60m arrival heights; we use 10m in the final analysis with 6 hourly steps. To compensate for the sparse meteorological

measurements, we calculate hourly trajectories and select those arriving at the hours: 00:00; 06:00; 12:00; and 18:00.

S.3.3 – The conclusions discussed in this section should be moved to S.4 and discussed in the context of the existing literature.

We tried to edit and move the sections, but the results and the discussion sessions had to kept separate due the large amount of material presented.

S.4.2 – The conclusions should be separated from the discussion. The work presented here is worthwhile and the main points should not be hidden.

We expanded this section and the conclusion section explaining further studies will address this intercomparison study.

Overall – consistency in figure references, especially for SI figures, should be double checked. E.g. Fig. SI 3 @ P.11 L11 vs Fig. SI3e @ P.11 L33).

Edited

Overall – references need to be double checked in both the main text and the references section.

Edited

References:

Rankin, A. M. and Wolff, E. W.: A year-long record of size-segregated aerosol composition at Halley, Antarctica, *J. Geo-phys. Res.*, 108, D244775,doi:10.1029/2003JD003993,2003.

Preunkert, S., Legrand, M., Jourdain, B., Moulin, C., Belviso, S., Kasamatsu, N., Fukuchi, M., and Hirawake, T.: Interannual variability of dimethylsulfide in air and seawater and its atmospheric oxidation by-products (methanesulfonate and sulfate) at Dumont d'Urville, coastal Antarctica (1999–2003), *J. Geophys. Res.*, 112, D06306, doi:10.1029/2006JD0075857, 2007.

Preunkert, S., Jourdain, B., Legrand, M., Udisti, R., Becagli, S., and Cerri, O.: Seasonality of sulfur species (dimethyl sulfide, sulfate, and methanesulfonate) in Antarctica: Inland versus coastal regions, *J. Geophys. Res. Atmos.*, 113, D15302,doi:10.1029/2008JD009937, 2008.

Saiz-Lopez, A., Mahajan, A. S., Salmon, R. A., Bauguitte, S. J. B., Jones, A. E., Roscoe, H. K., and Plane, J. M. C.: Boundary Layer Halogens in Coastal Antarctica, *Science*, 317, 348–351, 2007. Schmale, J., Schneider, J., Nemitz, E., Tang, Y. S., Dragosits, U., Blackall, T. D., Trathan, P. N., Phillips, G. J., Sutton, M., and Braban, C. F.: Sub-Antarctic marine aerosol: dominant contributions from biogenic sources, *Atmos. Chem. Phys.*, 13, 8669–8694, doi:10.5194/acp-13-8669-2013, 2013.

Giordano, M. R., Kalnajs, L. E., Avery, A., Goetz, J. D., Davis, S. M., and DeCarlo, P. F.:A missing source of aerosols in Antarctica – beyond long-range transport, phytoplankton, and photochemistry, *Atmos. Chem. Phys.*, 17, 1–20, <https://doi.org/10.5194/acp-17-1-2017>, 2017.

Interactive comment on “On the annual variability of Antarctic aerosol size distributions at Halley research station” by Thomas Lachlan-Cope et al.

Anonymous Referee #3

Received and published: 11 November 2019

Comments: Lachlan-Cope et al. present a novel study of Antarctic aerosol size distribution collected over a whole year of measurements at Halley research station. By applying the K-means clustering data analysis, eight aerosol categories were characterized. Based on the air mass back trajectory analysis, major sources regions including sea ice, open ocean, snow, and etc. were elucidated. Then, this study concluded that NPF and growth events in the Antarctic atmosphere mainly originated from both the sea ice marginal zone and the Antarctic plateau.

Many thanks for the appreciation of the paper.

The implication for climate and conclusion section is well-written, and in particular, the brief comparison with two other Antarctic stations (Dom C Concordia and King Sejong Station) during the year 2015 is a very useful and insightful section. Overall, the manuscript is generally well-written and interesting to read, with clear structure and sufficient explanations. The manuscript may be suitable to be published in Atmospheric Chemistry and Physics.

Many thanks for the appreciation of the paper.

Major Comments:

Page 2 and Lines 30: In the present study, cluster “pristine_160” with a bimodal size distribution (75 nm and 160 nm, respectively) shows the highest WS, but there were no correlations between them. Please clarify the meaning of “strong correlation in the abstract”.

Edited, associated

Page 11 and Lines 19: New particle formation and growth was observed for the nucleation mode PSC cluster. In addition, the authors mentioned that NPF and growth events originate from both sea ice marginal zone and the Antarctic plateau in the abstract. Please, calculate and suggest the growth rate, which is a critical factor that affects the CCN number concentration in Antarctic regions. Then, the value could be compared according to the air mass origins.

Growth rate were calculated for the NPF events detected

Page 15 and line 9. Almost 5 pages were partitioned to discussion section that was overlapped with introduction section. Most of the discussion section should be moved to introduction section and SI.

We tried to discuss our results and compare them with existing literature. That is why most of the more specific studies - for example primary and secondary aerosol sources - are discussed in the discussion section. The main issue is that we present here novel results from an entire year and we discuss aerosol sources and processes. We decided to leave a brief introduction section, and to provide a discussion of our results relative to the existing literature.

Page 20 and line 19. The authors compared data from Halley, Dome C, and King Sejong Station. Overall, much higher concentrations are seen at the coastal Antarctic sites relative to continental based Dome C station. The coastal Antarctic stations being a remote location might be not immune to man-made impacts and specific tracers (e.g., black carbon) are necessary to discern those influence. In particular, quite high BC concentration was detected in King Sejong Station, as presented by Kim et al. (2018). Here, the possible sources of NPF and growth due to human activity (anthropogenic influence) could be discussed.

We have a paper in preparation where aerosol size distribution data from the entire 2015 are analyzed all together. We edited the manuscript.

Minor Comments:

Page 9 and Line 1: Section 2.3 is missing.

Edited

Page 10 and Line 1: As mentioned in the manuscript, the difference between spring and autumn at $D_p > 60$ nm is very interesting. Please, explain possible reasons.

The difference between spring and autumn at $D > 60$ nm is also interesting, showing much higher concentrations in autumn, and likely due to a number of additional unknown sources including primary (sea spray) and secondary (sulphate and other components). Indeed clustering results in Figure 2 shows higher amounts of bimodal cluster and in general larger Aitken modes. Results are discussed in the discussion section.

Page 2 and Lines 30: Error should be displayed in Figure SI 5. Please, provide the relationships between total particle number concentration and each meteorological data (e.g., wind speeds, RH, T, and ozone) according to the different aerosol categories.

Error bars are generally 25%, not shown to emphasise different among different clusters.

Page 38 and line 6: What is meant by “Please note that the sea ice extent is the median September extent from 1981-2010” in Figure 7.

It is the median of the month of September, taken as average from the period 1981-2010.

1

2 **On the annual variability of**

3 **Antarctic aerosol size**

4 **distributions at Halley research**

5 **station**

6

7 Thomas Lachlan-Cope¹, David Beddows², Neil Brough¹, Anna E.
8 Jones¹, Roy M. Harrison^{2,+}, Angelo Lupi³, Young Jun Yoon⁴, Aki
9 Virkkula^{5,6} and Manuel Dall'Osto^{7*}

10

11 ¹*British Antarctic Survey, NERC, High Cross, Madingley Rd, Cambridge, CB3*
12 *0ET, United Kingdom*

13 ²*National Center for Atmospheric Sciences, University of Birmingham,*
14 *Edgbaston, Birmingham, B15 2TT, United Kingdom*

15 ³*Institute of Atmospheric Sciences and Climate (ISAC), National Research*
16 *Council (CNR), via P. Gobetti 101, 40129, Bologna Italy*

17 ⁴*Korea Polar Research Institute, 26, SongdoMirae-ro, Yeonsu-Gu, Incheon,*
18 *KOREA 406-840*

19 ⁵*Institute for Atmospheric and Earth System Research, University of Helsinki*
20 *Helsinki, FI-00014, Finland*

21 ⁶*Finnish Meteorological Institute, FI-00101 Helsinki, Finland*

22 ⁷*Institute of Marine Sciences, Passeig Marítim de la Barceloneta, 37-49. E-*
23 *08003, Barcelona, Spain; corresponding author, email: dallosto@icm.csic.es*

24

25 ⁺Also at: Department of Environmental Sciences/Centre of Excellence in
26 Environmental Studies, King Abdulaziz University, PO Box 80203, Jeddah,
27 21589, Saudi Arabia.

Abstract

Eliminado: ¶

The Southern Ocean and Antarctic region currently best represent one of the few places left on our planet with conditions similar to the preindustrial age. Currently, climate models have low ability to simulate conditions forming the aerosol baseline; a major uncertainty comes from the lack of understanding of aerosol size distributions and their dynamics. Contrasting studies stress that primary sea-salt aerosol can contribute significantly to the aerosol population, challenging the concept of climate biogenic regulation by new particle formation (NPF) from dimethyl sulphide marine emissions.

We present a statistical cluster analysis of the physical characteristics of particle size distributions (PSD) collected at Halley (Antarctica) for the year 2015 (89% data coverage, 6-209 nm size range, daily size resolution). By applying the Hartigan-Wong k-Means method we find 8 clusters describing the entire aerosol population. Three clusters show *pristine* average low particle number concentrations ($< 121-179 \text{ cm}^{-3}$) with three main modes (30 nm, 75-95 nm, 135-160 nm) and represent 57% of the annual PSD (up to 89-100% during winter, 34-65% during summer based upon monthly averages). Nucleation and Aitken mode PSD clusters dominate summer months (Sep-Jan, 59-90%), whereas a clear bimodal distribution (43 and 134 nm, respectively, min Hoppel mode 75 nm) is seen only during the Dec-Apr period (6-21%). Major findings of the current work include: (1) NPF and growth events originate from both the sea ice marginal zone and the Antarctic plateau, strongly suggesting multiple vertical origins, including marine boundary layer and free troposphere; (2) very low particle number concentrations are detected for a substantial part of the year (57%), including summer (34-65%), suggesting that the strong annual aerosol concentration cycle is driven by a short temporal interval of strong NPF events; (3) a unique pristine aerosol cluster is seen with a bimodal size distribution (75 nm and 160 nm, respectively), strongly associated with high wind speed and possibly associated with blowing snow and sea spray sea salt, dominating the winter aerosol population (34-54%). A brief comparison with two other stations (Dome C Concordia and King Sejong Station) during the year 2015 (240 days overlap) shows that the dynamics of aerosol number concentrations and

Eliminado: correlating

1 distributions are more complex than the simple sulphate-sea spray binary
2 combination, and it is likely that an array of additional chemical components
3 and processes drive the aerosol population. A conceptual illustration is
4 proposed indicating the various atmospheric processes related to the
5 Antarctic aerosols, with particular emphasis on the origin of new particle
6 formation and growth.

7

8 **1 Introduction**

9

10 Atmospheric marine aerosol particles contribute substantially to the global
11 aerosol budget; they can impact the planetary albedo and climate (Reddington
12 et al., 2017). However, aerosols remain the least understood and constrained
13 aspect of the climate system (Boucher et al., 2013). Aerosol concentration,
14 size distribution, chemical composition and dynamic behavior in the
15 atmosphere play a crucial role in governing radiation transfer. However,
16 aerosol sources and processes, including critical climate feedback
17 mechanisms, are still not fully characterized. This is especially true in pristine
18 environments, where the largest uncertainties are found, mainly due to lack of
19 understanding of pristine natural sources (Carslaw et al., 2013). Indeed, the
20 Southern Ocean and the Antarctic region still raises many unanswered
21 atmospheric science questions. This region has complex interconnected
22 environmental systems - such as ocean circulation, sea ice, land and snow
23 cover – which are very sensitive to climate change (Chen et al., 2009).

24 Early research upon Antarctic aerosols was carried out over various part of
25 the continent and reviewed by Shaw et al. (1988). It was concluded that a
26 peculiar feature of the Antarctic aerosol system is a very pronounced annual
27 cycle of the total particle number concentration, with concentrations 20-100
28 times higher during austral summer than during winter.

29 This seasonal cycle - like a seasonal "pulse" over the summer months
30 (December, January and February) - seems to be more prominent in the
31 upper Antarctic plateau than the coastal Antarctic zones, but particle number
32 concentrations are much higher in coastal Antarctica. One possible origin for
33 these nuclei could be the Antarctic free troposphere, as suggested by Ito et al.

1 (1993), although this free troposphere to marine boundary layer transport was
2 considered by no means a definite explanation (Koponen et al., 2002; 2003).
3 Overall, the aerosol summer maximum concentrations can be largely
4 explained by new particle formation (NPF) events, as recently reviewed by
5 Kerminen et al., (2018).

6 The vertical origin of these NPF events is still matter of debate. Some
7 indications suggesting NPF takes place preferentially in the Antarctic Free
8 Troposphere (FT): aerosols originate in the upper troposphere, then the
9 circulation induced by the Antarctic drainage flow (James, 1989) transports
10 aerosols down to the boundary layer in the Antarctic plateau, with subsequent
11 transport further to the coast by katabatic winds (Ito et al., 1993; Koponen et
12 al., 2002; Fiebig et al., 2014; Hara et al., 2011; Järvinen et al., 2013;
13 Humphries et al., 2016). A recent study found that the Southern Ocean was
14 the dominant source region for particles observed at Princess Elisabeth (PE)
15 station, leading to an enhancement in particle number (N), while the Antarctic
16 continent itself was not acting as a particle source (Herenz et al., 2019).
17 Further studies also point to boundary layer oceanic sources of NPF events
18 (Weller et al., 2011; Weller et al., 2015; Weller et al., 2018). Recently, a long
19 term analysis of the seasonal variability in the physical characteristics of
20 aerosol particles sampled from the King Sejong Station (located on King
21 George Island at the top of the Antarctic Peninsula) was reported (Kim et al.,
22 2017). The CCN concentration during the NPF period increased by
23 approximately 11 % compared with the background concentration (Kim et al.,
24 2019). Interestingly, new particle formation events were more frequent in the
25 air masses that originated from the Bellingshausen Sea than in those that
26 originated from the Weddell Sea, and it was argued that the taxonomic
27 composition of phytoplankton could affect the formation of boundary layer new
28 particles in the Antarctic Ocean (Jang et al., 2019). Dall'Osto et al. (2017)
29 reported higher ultrafine particles in sea ice-influenced air masses.

Eliminado: N

30
31 Overall, studies to date suggest that regional NPF events in Antarctica are not
32 as frequent as those in the Arctic or other natural environments, although the
33 growth rates are similar (Kerminen et al., 2018). In terms of aerosol size, most
34 of the ultrafine (<100 nm) particle concentrations have been linked to NPF

1 events, whereas sea salt particles dominate the coarse mode and
2 accumulation mode (>100 nm). A recent study by Yang et al. (2019), however,
3 proposes a source for ultrafine sea salt aerosol particle from blowing snow,
4 dependent on snow salinity. This mechanism could account for the small
5 particles seen during Antarctic winter at coastal stations.

6
7 It is interesting to note that the recent, spatially-extensive study of the
8 concentration of sea-salt aerosol throughout most of the depth of the
9 troposphere and over a wide range of latitudes (Murphy et al., 2019) reported
10 a source of sea-salt aerosol over pack ice that is distinct from that over open
11 water, likely produced by blowing snow over sea ice (Huang et al., 2018;
12 Giordano et al., 2018; Frey et al., 2019). In recent years, a number of long
13 term aerosol size distribution datasets have been discussed (Järvinen et al.,
14 2013; Kim et al., 2019) but these types of datasets are still scarce. The ability
15 to measure aerosol size distributions at high time resolution allows open
16 questions to be investigated. The purpose of the present work is to examine
17 for the first time a one year long (2015) dataset collected at Halley Station.

18
19 Previous work at the Halley research station reported size-segregated aerosol
20 samples collected with a cascade impactor at 2 week intervals for a year. Sea
21 salt was found to be a major component of aerosol throughout the year (60%
22 of mass) deriving from the sea ice surface rather than open water.
23 Methanesulphonic Acid (MSA) and non-sea-salt sulphate both peaked in the
24 summer and were found predominantly in the submicron size range (Rankin
25 and Wolff, 2003). Observations of new particle formation during a two month
26 cruise in the Weddell Sea revealed an iodine source (Atkinson et al., 2012).
27 While no short-term correlation (timescale < 2 days) was found between
28 particles and iodine compounds in a later study (Roscoe et al., 2015), the
29 authors highlighted correlations on seasonal timescales. It is also worth
30 mentioning that a previous Weddell Sea study also found increased new
31 particle formation in the sea ice zone (Davison et al., 1996), but no clear
32 correlation between dimethyl sulphide and new particle bursts was found.

33

1 In this paper, we use k-means cluster analysis (Beddows et al., 2009) to
2 elucidate the properties of the aerosol size distributions collected across the
3 year 2015 at Halley. A clear advantage of this clustering method over
4 average size distributions (e.g. monthly, seasonally, etc.) is that specific
5 aerosol categories of PSD can be compared across different time periods, as
6 further described later in section 2. While a number of intensive polar field
7 studies have focused on average monthly datasets, cluster analyses of year
8 long polar and marine particle size distributions measurements are scarce. In
9 a nutshell, these clustering method can reduce the complexity of the PSD
10 dataset, allowing an smoother separation of different PSDs (Beddows et al.,
11 2014). Recently, cluster analysis was applied to Arctic aerosol size
12 distributions taken at Zeppelin Mountain Svalbard; Dall'Osto et al., 2017a)
13 during an 11-year record (2000–2010) and at Villum Research Station
14 (Greenland; Dall'Osto et al., 2018b) during a 5-year period (2012–2016). Both
15 studies showed a striking negative correlation between sea ice extent and
16 nucleation events, and concluded that NPF are events linked to biogenic
17 precursors released by open water and melting sea ice regions, especially
18 during the summer season. Recently, data from three high Arctic sites
19 (Zeppelin research station, Gruevbadet Observatory, Villum Research Station
20 at Station Nord) over a 3-year period (2013–2015) were analysed via
21 clustering analysis, reporting different categories including pristine low
22 concentrations (12%–14% occurrence), new particle formation (16%–32%),
23 Aitken (21%–35%) and accumulation (20%–50%) particles categories
24 (Dall'Osto et al., 2019). To our knowledge, this is the first year-long Antarctic
25 dataset where cluster analysis has been applied. The objective of this work is
26 to analyze different types of aerosol size distributions collected over a whole
27 year of measurements, to elucidate source regions (including open ocean,
28 land, snow on land, consolidated and marginal sea ice zones), discuss
29 possible primary and secondary aerosol components, and propose
30 mechanisms where NPF and growth may take place in the study region.

31
32
33
34

Eliminado: ¶

2. Methods

2.1 Location

The measurements reported here were made at the British Antarctic Survey's Halley VI station (75° 36'S, 26° 11'W), located in coastal Antarctica, on the floating Brunt Ice Shelf ~20 km from the coast of the Weddell Sea. A variety of measurements were made from the Clean Air Sector Laboratory (CASLab), which is located about 1 km south-east of the station (Jones et al., 2008).

2.2 SMPS and CPC

The aerosol size distribution was measured using a TSI Inc. Scanning Mobility Particle Sizer (SMPS), comprising an Electrostatic Classifier (model 3082), a Condensation Particle Counter (CPC) model 3775, and a long Differential Mobility Analyser (DMA, model 3081). The SMPS returned information on numbers of particles in discrete size bins in the size range 6 nm to 209 nm, at 1-min temporal resolution. A condensation particle counter (CPC, TSI Inc. model 3010) is routinely run at Halley. It provides a measure of total number of particles with diameter between 10 nm and ~3 microns. Both instruments sampled from the CASLab's central, isokinetic, aerosol stack (200 mm i.d. stainless steel) (see Jones et al. (2008) for details).

2.2.1. SMPS K means clustering data analysis

Cluster Analysis has routinely been used to understand SMPS data for over a decade (Dall'Osto et al (2019, 2018a, 2018b, 2018c, 2017, Lange et al 2018, Beddows et al 2014, 2009) and is useful in reducing the complexity of multivariate data into a manageable size to understand natural processes in the environment. The cluster analysis procedure is relatively straightforward and consists of three stages: (i) normalisation; (ii) cluster choice; and (iii) cluster partition.

Con formato: Interlineado:
1,5 líneas

Con formato: Fuente:
(Predeterminado) Arial

1 (i) Prior to clustering, the SMPS distributions are normalized so that the
2 Euclidean length of each (treated as a vector) is 1. This ensures
3 that we are clustering the shape of the distributions irrespective of
4 the magnitude of the number count within each. The normalized
5 data given then are clustered using *k*-means (method R Core Team
6 (2019). This partitions the SMPS distributions (treated as vectors by
7 *k*-means) into *k* groups such that the sum of squares of the
8 distances from these points to the assigned cluster centres is
9 minimized. At the minimum, the cluster centres form the average
10 SMPS distributions of the individual SMPS distributions assigned to
11 each cluster (see supporting information in Beddows and Harrison,
12 2019 for more details).

Con formato: Numeración y viñetas

13 (ii) The choice of cluster number can be decided upon using cluster
14 validation metrics which parameterise the compactness and
15 separation of the clusters within the measurements space (i.e. a
16 space with the same number of dimensions as the number of size
17 bins within the SMPS). In an ideal case, each cluster forms its own
18 island within the measurement space, defined by highly similar
19 elements (i.e. are compact) and are distinct from each other by
20 highly dissimilar elements (i.e. are separate). However, in the case
21 of SMPS spectra such a high degree of compactness and
22 separation is not realised in environmental data. Instead, the data is
23 partitioned into areas of increased density within the measurement
24 space, i.e. the data does not have sufficient compactness and
25 separation to form *islands* within the measurement space but
26 instead forms *hills* within the measurement *landscape*, which is
27 divided up by the partitions.

Con formato: Fuente: (Predeterminado) Arial

Con formato: Fuente: (Predeterminado) Arial

Con formato: Espacio Después: 8 pto, Interlineado: 1,5 líneas, Numerado + Nivel: 1 + Estilo de numeración: i, ii, iii, ... + Iniciar en: 1 + Alineación: Izquierda + Alineación: 0.63 cm + Tabulación después de: 0 cm + Sangría: 1.9 cm

28
29 To decide on the number of factors, the Dunn Index (DI) and Silhouette
30 Width (SW) were calculated for each factor number (Halkidi et al 2001 and
31 Rousseeuw 1987). The DI is a function the ratio of the smallest distance
32 between observations not in the same cluster to the largest intra-cluster
33 distance. Hence, DI has a value of 0 and above. The higher the values
34 the more compact and separate are the elements within the clusters but

Con formato: Sangría: Izquierda: 0.63 cm, Espacio Después: 8 pto, Interlineado: 1,5 líneas

Con formato: Fuente: (Predeterminado) Arial

1 conversely the closer the value is to zero the more loose and diffuse the
2 elements are across the clusters. When cluster analysing SMPS data, a
3 DI of the order of 10^{-3} - 10^{-4} is often obtained indicating that *k*-Means is
4 partitioning the data into clusters which are in close proximity to each other.

Con formato: Sangría:
Izquierda: 0.63 cm,
Interlineado: 1,5 líneas

5
6 The average SW value is a measure of how similar the observations are
7 with the clusters they are assigned to relative to other clusters. A value
8 approaching 1 indicates that the elements within each cluster are identical
9 to each other; a values close to 0 suggest that there is no clear division
10 between clusters; and a value to -1 suggest that elements are better
11 placed in its nearest neighbouring cluster. Typical values for SMPS data
12 are of the order 0.3 - 0.4, and coupled with the low DI value, indicate that
13 the clusters within the SMPS data are less compact and separate but
14 rather loose and diffuse (cf the analogy alluded to above of *hills within a*
15 *landscape* instead of *island within a sea*).

Con formato: Fuente:
(Predeterminado) Arial

16
17 As we increase the cluster number from 2 up to 30, the SW value
18 decreases from a maximum value of 0.49 to 0.28 and the DI increases
19 from a minimum of 2.9×10^{-3} to a maximum 12.3×10^{-3} (Figure SI 1). As
20 the number of clusters is increased from 2, the increase in DI and
21 decrease in SW reflects the 'loose and diffuse' nature of the SMPS
22 elements within the clusters, i.e. as the number of clusters is increase, the
23 small irregularities within the data due to noise, are more likely to be
24 partitioned. Hence, we look for the cluster number (in this case 8 cluster;
25 with SW = 0.35 and DI = 4.6×10^{-3}) where there is a peak in this trend
26 identifying the natural partition within the data, which marks out the *islands*
27 of increased density space.

Con formato: Fuente:
(Predeterminado) Arial

28
29 As with all statistical methods, there is a tendency to depend on the cluster
30 validation metrics to drive the final solution that may not necessarily be the
31 correct solution to describe the environmental conditions. Hence, they are
32 only used as a guide and it is often helpful as a next step to compare the
33 plots of the individual SMPS elements against the mean SMPS of each
34 cluster (Figure SI 2).

Con formato: Sangría:
Izquierda: 0.63 cm,
Interlineado: 1,5 líneas, Sin
viñetas ni numeración

Con formato: Fuente:
(Predeterminado) Arial

Con formato: Fuente:
(Predeterminado) Arial

1
2 From figure SI 2, it is clear that we do indeed have sufficient separation of
3 the SMPS data within the clusters with the odd spurious NSD in clusters 1,
4 3, 4 and 7, which are themselves insufficient in number to form their own
5 cluster, but are allocated to their nearest cluster. From this optimum
6 situation, it can envisioned that as we reduce the number of clusters we
7 will lose the integrity of the separation and we might well expect the cluster
8 elements to aggregate into larger clusters according to their modal
9 diameter, eg Clusters 1, 3, 4 and 7; clusters 2, 6 & 8; and cluster 6. In fact,
10 when we calculate the median standard deviation of the SMPS data within
11 the clusters for 2-10 clusters, there is in fact a minimum value at 8 clusters
12 thus further supporting our cluster partitions.

Con formato: Sangría:
Izquierda: 0.63 cm,
Interlineado: 1,5 líneas

Con formato: Fuente:
(Predeterminado) Arial

Con formato: Interlineado:
1,5 líneas

Eliminado: ¶
Prior to clustering, the SMPS distributions are normalized so that the Euclidean length of each (treated as a vector) is 1. This ensures that we are clustering the shape of the distributions irrespective of the magnitude of the number count within each. The normalized data given then are clustered using the k-means (method R Core Team (2019)). This partitions the SMPS distributions (treated as vectors by k-means) into k groups such that the sum of squares of the distances from these points to the assigned cluster centres is minimized. At the minimum, the cluster centres form the average SMPS distributions of the individual SMPS distributions assigned to each cluster.¶

¶
To decide on the number of factors to choose, the Dunn Index and Silhouette Width were calculated for each factor number. The Dunn Index is the ratio of the smallest distance between observations not in the same cluster to the largest intra-cluster distance. The Dunn Index has a value between zero and infinity, and should be maximized. Similarly, the Silhouette Width analysis is a measure of how similar the observations are with the cluster they are assigned to relative to other clusters. Its value ranges from -1 to 1 for each observation in your data. A value approaching 1 indicates that the elements within each cluster are identical to each other; a values close to 0 suggest that there is no clear division between clusters; and a value to -1 suggest that the observations have been assigned to the wrong cluster. As we increase the cluster number from 2 up to 30 the Silhouette Width falls from a maximum value of 0.49 to 0.28 and the Dunn Index increases from a minimum of 2.9×10^{-3} to a maximum 12.3×10^{-3} . As the number of clusters is increased from 2, the increase in Dunn Index reflects the sequen ... [1]

2.3 Meteorological data

15 Standard meteorological measurements are made at the new Clean Air
16 Sector Laboratory (CASLab) which is designed specifically for studies of
17 background atmospheric chemistry and air/snow exchange, further
18 information can be found elsewhere (Jones et al., 2008; Vignon et al., 2019).

2.4 Air mass trajectories

23 Air mass backtrajectories were calculated using the HYSPLIT4 trajectory
24 model (Draxler and Hess, 1998) using the NCAR/NCEP 2.5-deg global
25 reanalysis archive (Kalnay et al., 1996). Trajectories were calculated arriving
26 at Halley (Lat. 75°34'16"S, Long. 25°28'26"W, 30m above sea level (asl))
27 every 6 hours (06:00, 12:00, 18:00, 00:00) during the study period. All
28 calculations were carried out through the Openair trajectory functions in Cran
29 R (Carslaw and Ropkins 2012). In particular, once calculated, the trajectories
30 were clustered using the Openair function *trajCluster* using the Euclidean
31 method. When considering the various cluster numbers, a setting of 6
32 trajectory clusters were chosen as best describing the air masses arriving at
33 Halley. Note that metrics similar to the Dunn Index and Silhouette Width were
34 not needed in this decision. The results of the air mass trajectory calculation

Eliminado: and other

1 were plotted either as individual, average or raster layer objects (Hijmans
2 (2019)) drawn on stereographic projections of Antarctica using the *mapproj*
3 and *maps* package (Becker 2018, Doug McIlroy *et al* 2018).

3. Results

3.1 Categorizing Antarctic aerosol size distributions

3.1.1 Average particle number and size resolved concentrations

11 We investigated the seasonal variability in the physical aerosol size
12 characteristics of particles sampled from Halley VI Station in coastal
13 Antarctica over the period January to December 2015. A clear maximum at 45
14 nm and at 145 nm can be seen in the annual average size distribution (Fig. 1).
15 However, a striking difference can be seen among different seasons: high
16 concentrations of aerosols at about 40 nm dominate during summer, whereas
17 larger modes can be observed during winter; with intermediate conditions
18 during spring and autumn. The difference between spring and autumn at
19 $D > 60$ nm is also interesting, showing much higher concentrations in autumn,
20 and likely due to a number of additional unknown sources including primary
21 (sea spray and blowing snow) and secondary (sulphate and organic
22 components). Results are broadly in line with previous results published from
23 the Antarctic Peninsula (Kim *et al.*, 2017). Total particle number
24 concentrations are derived from a condensation particle counter (CPC)
25 deployed parallel to the SMPS (Fig. SI 3), supporting the excellent
26 performance of the SMPS over a large data coverage (89% of the time during
27 2015). Minimum concentrations are found for the month of August (47 ± 10 cm⁻³)
28 and maximum for January (602 ± 65 cm⁻³). These are reflected in the clear
29 seasonal cycles for the total particle concentration (CN) observed (Fig SI 4).
30 Figure SI 4 (bottom) also shows daily average concentrations of the $N_{30 \text{ nm}}$,
31 $N_{30-100 \text{ nm}}$ and $N_{>100 \text{ nm}}$ integral particle population. The selected cutoffs of 30
32 and 100 nm are based on the average shape of the size distribution (Figure 1).
33 It is interesting that whereas the absolute concentrations are remarkably

Eliminado: .

Eliminado: R

Eliminado: 1

Eliminado: 2

Eliminado: 2

1 different, the relative percentages of the three aerosol populations do not
2 differ much across different months, on average $21\pm 9\%$, $54\pm 7\%$ and $25\pm 8\%$
3 for the $N_{30\text{ nm}}$, $N_{30-100\text{ nm}}$ and $N_{>100\text{ nm}}$, respectively. Ultrafine particles dominate
4 summer concentrations, but are - relative to total - a dominating fraction also
5 during winter.

6

7 **3.1.2 K-means SMPS cluster analysis**

8

9 K-means cluster analysis of particle number size distributions was performed
10 using 5,664 hourly distributions collected over the year of 2015. Our clustering
11 analysis led to an optimum number of eight categories of aerosol number size
12 distributions. The corresponding average daily aerosol number size
13 distributions are shown in Figure 2a, whereas the annual seasonality is shown
14 in Figure 2b. Here, we refer to ultrafine as particles with diameters between 6
15 and 210 nm. Three categories were characterized by very low particle number
16 concentrations ($<200\text{ particles cm}^{-3}$), and described by their different aerosol
17 modes (plotted and size resolved in Fig. 3), specifically:

18

19 - "*Pristine_30*" ultrafine. Occurring annually 19% of the time (min-max 0-55%
20 based on monthly averages), this aerosol category ($N_{\text{CPC}} 179\pm 30\text{ cm}^{-3}$) shows
21 two main peaks at 30 nm and 95 nm (Fig. 3, Fig. SI 5). The maximum in
22 occurrence is seen for the months of September (47%) and May (55%).

Eliminado: 3

23

24 - "*Pristine_75*" ultrafine. Occurring annually 29% of the time (min-max 0-61%
25 based on monthly averages), this aerosol category ($N_{\text{CPC}} 157\pm 25\text{ cm}^{-3}$) shows
26 two main peaks at 70 nm and 130 nm (Fig. 3, Fig. SI 5). The occurrence is
27 scattered across all year except during spring months (Sept/Oct).

Eliminado: 3

28

29 - "*Pristine_160*" ultrafine. Occurring annually 9% of the time (min-max 0-52%
30 based on monthly averages), this aerosol category ($N_{\text{CPC}} 121\pm 40\text{ cm}^{-3}$) shows
31 two main peaks at 70 nm and 160 nm (Fig. 3, Fig. SI 5). The maximum in
32 occurrence is seen for the winter months of June (41%) and July (52%).

Eliminado: 3

33

1 These three pristine aerosol cluster types describe up to 57% of the aerosol
2 population, and mainly dominate the aerosol population during cold months
3 (73%-100% for Apr-Aug.) Other aerosol categories possessing higher particle
4 concentrations include:

5
6 - "*Nucleation*" ultrafine. Occurring annually 3% of the time (min-max 0-11%
7 based on monthly averages), this aerosol category ($N_{CPC} 620 \pm 220 \text{ cm}^{-3}$)
8 shows a main nucleation peak at 15 nm detected during summer months (Fig.
9 2 a, b). Figure [SI5d](#) shows the evolution of the aerosol number size
10 distributions starting at about noon and peaking at about 18:00; overall 95% of
11 these events were detected during daylight. The name of this category - which
12 will be used below to represent new particle formation events - stands for
13 continuous gas-to-particle growth occurring after the particle nucleation event,
14 although these nucleation events - detected at about 7-10 nm - must have
15 originated away from the Halley station.

Eliminado: SI3d

16
17 - "*Bursting*" ultrafine. Occurring annually 9% of the time (min-max 0-37%
18 based on monthly averages), this aerosol category ($N_{CPC} 602 \pm 120 \text{ cm}^{-3}$)
19 shows a main nucleation peak at 27 nm detected during summer months (Fig.
20 2a, b). Fig. [SI5e](#) suggests these aerosols are similar to the *Nucleation* cluster,
21 although these new particle formation events are already in the growth
22 process almost reaching 30 nm on average.

Eliminado: 3

23
24 Clusters *Nucleation* and *Bursting* are seen during summer months and
25 September-October, contributing up to 44% of the total aerosol population
26 during the months of September and January (Fig. [SI6b, d](#)). Following
27 terminology developed in previous work (Dall'Osto et al., 2017, 2018) the
28 remaining aerosol clusters can be classified as followed:

Eliminado: 4

29
30 - "*Nascent*" ultrafine. This category occurs annually 10% of the time, with a
31 strong seasonal trend peaking during summer (October-December, 10-39%)
32 and with a broad Aitken mode centred at about 38 nm (Fig.2) without showing
33 a clear diurnal pattern (Fig. [SI5f](#)). The name of this category emerges from

Eliminado: 3

1 growing ultrafine aerosol particles which may result from an array of different
2 primary and secondary aerosol processes.

3
4 - "Aitken" ultrafine. This category occurs annually 15% of the time, with a
5 strong seasonal trend peaking during summer (Oct-Dec, 32-63%, Fig. 2b) and
6 - similar to the *Nascent* cluster - a broad Aitken mode centred at about 50 nm
7 (Fig 2a) without showing a clear diurnal pattern (Fig. SI 5h).

8
9 - "Bimodal" ultrafine. Occurring annually 5% (min-max 0-21%) of the time, this
10 unique category shows a strongly bimodal size distribution (43nm and 134nm,
11 with a small nucleation mode at 16 nm, Fig. 2 a), it occurs during the period
12 Dec-Apr (7-21%) and parallels previously reported bimodal aged Antarctic
13 distributions (Ito et al., 1993). The minimum of the Hoppel mode is seen at 70
14 nm.

15
16 In summary, our method allows apportionment of the Antarctic aerosol
17 observed at Halley research station into eight categories describing the whole
18 aerosol population. In the following sections, emphasis is given to
19 understanding the origin and processes driving Antarctic aerosol formation.

20 21 **3.2 Association of PSD with meteorological, physical and chemical** 22 **parameters**

23
24 The main ground-level meteorological observations from Halley for the year
25 2015 are temporally averaged over the periods of occurrence of the different
26 aerosol categories (Fig SI 7). Higher average wind speeds (WS, $7.2 \pm 2 \text{ m s}^{-1}$)
27 were encountered for the pristine aerosol clusters relative to the remaining
28 five ($3.2 \pm 2 \text{ m s}^{-1}$); cluster *pristine 160* shows the highest WS ($8.5 \pm 3 \text{ m s}^{-1}$),
29 suggesting the larger mode may be due to a primary aerosol component,
30 further discussed in Section 4. Little variation in atmospheric pressure was
31 found among the eight aerosol clusters. By contrast, *Nucleation* and *Bursting*
32 clusters were found in driest (Relative Humidity RH, $48 \pm 5\%$) and coldest (T -
33 $17 \pm 0.2 \text{ }^\circ\text{C}$) weather among all clusters, supporting the fact that NPF takes
34 place preferentially at low RH (Laaksonen et al.; 2009; Hamed et al. 2011).

Eliminado: 3

Eliminado: The main ground-level meteorological observations from Halley for the year 2015 are temporally averaged over the periods of occurrence of the different aerosol categories (Fig SI 5). Higher average wind speeds (WS, $7.2 \pm 2 \text{ m s}^{-1}$) were encountered for the pristine aerosol clusters relative to the remaining five ($3.2 \pm 2 \text{ m s}^{-1}$); cluster *pristine_160* shows the highest WS ($8.5 \pm 3 \text{ m s}^{-1}$), suggesting the larger mode may be due to a primary aerosol component, further discussed in Section 4. Little variation in atmospheric pressure was found among the eight aerosol clusters. By contrast, *Nucleation* and *Bursting* clusters were found in driest (Relative Humidity RH, $48 \pm 5\%$) and coldest (T $-17 \pm 0.2 \text{ }^\circ\text{C}$) weather among all clusters, supporting the fact that NPF takes place preferentially at low RH (Laaksonen et al.; 2009; Hamed et al. 2011). ¶
Vertical profiles of meteorological data are available for most days in 2015, and complement local ground-level measurements. Fig. SI6a-b show driest and coldest conditions for clusters *Bursting* and *Nucleation*. By contrast, warmest and wettest conditions occur for the *Bimodal* category. A large difference is also seen in the wind speed vertical profiles (Fig. SI 6c), which are strongest for cluster *pristine_160*, and a clear inversion is seen during the *bimodal* cluster days. Concurrent ozone gas measurements (Fig. SI 5) show lowest values for the cluster *bimodal* ($18 \pm 3 \text{ ppb}$), moderate for ultrafine dominating clusters ($24 \pm 8 \text{ ppb}$), and higher values for pristine clusters ($29 \pm 5 \text{ ppb}$). ¶

1 Vertical profiles of meteorological data are available for most days in 2015,
2 and complement local ground-level measurements. Fig. SI6a-b show driest
3 and coldest conditions for clusters *Bursting* and *Nucleation*. By contrast,
4 warmest and wettest conditions occur for the *Bimodal* category. A large
5 difference is also seen in the wind speed vertical profiles (Fig. SI 8c), which
6 are strongest for cluster *pristine 160*, and a clear inversion is seen during the
7 *bimodal* cluster days. Concurrent ozone gas measurements (Fig. SI 7) show
8 lowest values for the cluster *bimodal* (18 ± 3 ppb), moderate for ultrafine
9 dominating clusters (24 ± 8 ppb), and higher values for pristine clusters (29 ± 5
10 ppb).

12 **3.3 Elucidating source regions by association of PSD clusters with air** 13 **mass back trajectories**

14
15 Throughout the studied period, hourly 120 h back trajectories were calculated
16 using the HYSPLIT4 model (Draxler and Hess, 1998). Figure 4 shows the
17 results of the air mass back trajectories calculated for Halley throughout 2015,
18 showing six main clusters. Broadly, two air trajectory clusters were associated
19 with anticyclonic conditions (clusters 2 and 6, up to 33.6% of air masses);
20 three clusters were associated with air masses coming from the East Antarctic
21 Plateau (clusters 3, 4, 5, up to 57.2% of air masses); and one unique air
22 trajectory cluster was found associated with air masses originating within the
23 Weddell Sea (cluster 1, 9%). Fig. SI9 shows the six air mass back trajectory
24 clusters and the average height of the trajectories up to 120 hours before
25 arrival at Halley. While clusters 2-6 show their origin over the Antarctic plateau,
26 cluster 1 shows average altitudes lower than 1000m, close to the height of the
27 mixed layer (Fig. SI9). Figure SI 10 shows the air mass trajectories according
28 to the PSD clusters. On the basis of Figure SI9, it looks rather similar to the
29 other air mass types with the air only entering the boundary layer for the last
30 ~15 hours of the trajectory. One striking difference is found when these air
31 mass back trajectory clusters are compared temporally among the aerosol
32 categories (Figure 5). A key conclusion of this study is that most aerosol
33 categories (excluding cluster *Nucleation*) are associated with air masses
34 arriving with Eastern winds from the Antarctic plateau (East short, East long,

Eliminado: 7

Eliminado: 7

Eliminado: 7

Eliminado: ¶

1 56-76% of the time). Anticyclones also seem to be a predominant air mass
2 type (17-42%). At Halley, air mass back trajectories that have travelled over
3 the sea/sea ice zone, play only a minor overall role in terms of annual average
4 air mass trajectories (10-15%). In a further analysis, we obtained information
5 on how far each air mass travelled (total travel time 60 h) over zones
6 distinguished by their surface characteristics, namely snow, sea ice and open
7 water for each one of the different aerosol categories presented (see
8 methods). Fig. 5a shows that category *Nucleation* is the one most associated
9 with sea ice (27% of the time). An example of a NPF events is shown in Fig.
10 SI 11, occurring on the 28th January 2015, where air masses back trajectories
11 showed most of their travel time over sea ice (65% consolidate, 25% open
12 pack, total 85%) and the remaining open ocean (10%). Further studies will
13 address specific events and more specific case studies. It is important to
14 stress that the *Nucleation* category has its air mass back trajectories mainly
15 travelling over land (63%). However - relative to the other clusters - it is the
16 most affected by air masses which had travelled over the Weddell Sea (27%),
17 most of which is open pack ice (ratio open pack / consolidated sea ice of 0.6,
18 Fig. 5b). This is an important conclusion of this work, pointing out that at least
19 two source regions of new particle formation exist in the Antarctic. It is
20 interesting to note also that the *Bursting* category has a large ratio of open
21 pack / consolidated sea ice (Fig 5b), confirming marginal sea ice zones may
22 be a strong source of biogenic gases responsible for new particle formation.
23 By examining the air mass trajectory heights, we also show that during the 5
24 days prior to sampling, the sampled air from the Weddell Sea was remarkably
25 different from the other air mass types (Fig. SI 9); it had travelled within the
26 marine boundary layer, with no intrusion from the free troposphere. Our
27 results strongly suggest the nucleating events originated within the boundary
28 layer, likely from gaseous precursors associated with sea ice emissions.

Eliminado: It is important to stress that the *Nucleation* category has its air mass back trajectories mainly travelling over land (63%). However - relative to the other clusters - it is the most affected by air masses which had travelled over the Weddell Sea (27%), most of which is open pack ice (ratio open pack / consolidated sea ice of 0.6, Fig. 5b).

Eliminado: 7

4. Discussion

4.1 Origin and sources of Antarctic aerosol

1
2 The purpose of this study was to analyze a year-long (throughout 2015) set of
3 observations of Antarctic aerosol number size distributions to gain a better
4 understanding of those processes which control Antarctic aerosol properties.
5 In a pristine environment like Antarctica and its surrounding ocean, where the
6 atmosphere is thought to still resemble that of preindustrial Earth (Hamilton et
7 al., 2014), missing aerosol sources must reflect overlooked natural processes.
8 Uncertainties for modeling aerosol-cloud interactions and cloud radiative
9 forcing arise from a poor source apportionment of aerosols and their size
10 distributions (Carslaw et al 2013).

11 Broadly, marine particles in the nanometer size range originate from gas-to-
12 particle secondary processes, whereas those in super-micron sizes are
13 predominantly composed of primary sea-spray (O'Dowd et al., 1997).
14 However, the accumulation mode (broadly composed of intermediate particle
15 sizes of 50 –500 nm) is composed of a complex mixture of both secondary
16 and primary particles. The relative roles of secondary aerosols produced from
17 biogenic sulfur versus primary sea-spray aerosols in regulating cloud
18 properties and amounts above the Southern Ocean is still a matter of debate
19 (Meskhidze and Nenes, 2006; Korhonen et al., 2008; Quinn and Bates, 2011;
20 Mc Coy et al., 2015; Gras and Keywood, 2017; Fossum et al., 2018). First
21 observations of organic carbon (OC) in size-segregated aerosol samples
22 collected at a coastal site in the Weddell Sea (Virkkula et al., 2006) showed
23 that MSA represented only a few % of the total OC in the submicron fraction;
24 recent studies demonstrate that sea bird colonies are also important sources
25 of organic compounds locally (Schmale et al., 2013; Liu et al., 2018) and from
26 seasonal ice microbiota (Dall'Osto et al., 2017). The overall balance between
27 secondary aerosol formation versus primary particle formation from sea spray
28 still needs to be determined and is a pressing open question.

29
30 A key result of this study is that for 59% of the year (89-100% during winter
31 JJA; 10-50% during spring SON; 34-65% during summer DJF; 48-91% during
32 autumn MAM), aerosol size distributions were characterized by very low
33 particle number concentrations ($< 121\text{-}179\text{ cm}^{-3}$). It is often assumed that a
34 strong annual cycle of particle number concentrations is mainly driven by

1 summer new particle formation events (Shaw, 1988; Ito et al., 1993; Kerminen
2 et al., 2018). However, at Halley during summer 2015, 34-65% of the time low
3 particle number concentrations (121-179 cm⁻³) of unknown origin dominate
4 the overall temporal variation. Unique bimodal size distributions are seen in
5 December-April, where a clear bimodal distribution is seen for 7-21% of the
6 time (peaking in March, 21%), and likely related to cloud processing (Hoppel
7 et al., 1994).

8 In the following sub-sections we discuss our results in the light of recent
9 studies focusing on Antarctic aerosol source apportionment. The majority of
10 the studies report primary and secondary components in term of mass, which
11 should not be confused with particle number concentration.

Eliminado: The majority of the studies report primary and secondary components in term of mass, which should not be confused with particle number concentration. ¶

12

13 **4.1.1 Primary Antarctic aerosol**

14

15 Sea spray is almost always reported as the main source of supermicron (>1
16 µm) aerosols in marine areas, including the Southern Ocean and Antarctica
17 (Quinn et al., 2015; Bertram et al., 2018). However, models of global sea-salt
18 distribution have frequently underestimated concentrations at polar locations
19 (Gong et al., 2002). Rankin and Wolff (2003) suggested the Antarctic sea ice
20 zone was a more important source of sea salt aerosol, during the winter
21 months, than the open ocean. In particular, they proposed brine and frost
22 flowers on the surface of newly forming sea ice as the dominant source, a
23 hypothesis supported by other studies (e.g. Udasti et al., 2012). The results
24 presented here suggest that, in coastal Antarctica, aerosol composition is a
25 strong function of wind speed and that the mechanisms determining aerosol
26 composition are likely linked to blowing snow (Giordano et al., 2019; Yang et
27 al., 2019; Frey et al., 2019). We note that Legrand et al. (2017a) suggested
28 that on average, the sea-ice and open-ocean emissions equally contribute to
29 sea-salt aerosol load of the inland Antarctic atmosphere.

30 Averaged across the year, we found a very clear aerosol size distribution with
31 the largest detected mode at ~160 nm, pointing to a primary - likely sea spray
32 - source, which was detected during periods of strong winds. However, it is
33 also possible that in size range the dominating constituent is sulphate (Teinilä
34 et al., 2014), further studies are needed to apportion this mode correctly. This

1 aerosol category type occurs very frequently during winter months (JJ, 33-
2 52%), but not during the other months (0-14%). Gras and Keywood (2017)
3 showed, using data from Cape Grim, that wind-generated coarse-mode sea
4 salt is an important CCN component year round and from autumn through to
5 mid-spring is the second most important component, contributing around 36%
6 to observed CCN; these measurements were taken in the Southern Ocean
7 marine boundary layer.

8 Marine primary organic aerosol (POA) is often associated with sea-spray, but
9 recent studies indicate that a fine mode (usually <200 nm) can have a size
10 distribution that is independent from sea-salt (externally mixed), whereas
11 supermicron marine aerosols are more likely to be internally mixed with sea-
12 salt (Gantt and Meskhidze, 2013). McCoy et al. (2015) reported observational
13 data indicating a significant spatial correlation between regions of elevated
14 Chl-a and particle number concentrations across the Southern Ocean, and
15 showed that modeled organic mass fraction and sulphate explains $53 \pm 22\%$
16 of the spatial variability in observed particle concentration. Our study cannot
17 apportion any aerosol related to primary organic aerosol, given the lack of
18 chemical measurements carried out during 2015 at Halley research station. It
19 is possible that part of the broad mode at 90 nm of the Pristine_90 category
20 contain a fraction of primary marine organic aerosols, but the relative
21 importance cannot be quantified in this study. Interestingly, open ocean
22 aerosol measurements collected over the Southern Ocean (43°S–70°S) and
23 the Amundsen Sea (70°S–75°S) were recently reported by Jung et al. (2019).
24 During the cruise, Water Insoluble Organic Components (WIOC) was the
25 dominant Organic Carbon (OC) species in both the Southern Ocean and the
26 Amundsen Sea, accounting for 75% and 73% of total aerosol organic carbon,
27 respectively. The WIOC concentrations were found to correlate with the
28 relative biomass of a specific phytoplankton species (*P. Antarctica*), producing
29 extracellular polysaccharide mucus and strongly affecting the atmospheric
30 WIOC concentration in the Amundsen Sea (Jung et al., 2019).

31

32 **4.1.2 Secondary Antarctic aerosol**

33

1 Our results show that two sub 30 nm aerosol categories (*Nucleation* and
2 *Bursting*, 12% in total) and two Aitken 30-60 nm aerosol categories (*Nascent*
3 and *Aitken*, 25%) account for up to 37% of the PSD detected during at Halley
4 the year 2015. Our results point to secondary aerosol processes driving the
5 aerosol population during five months of the year (Sep-Jan, 48-90%), where
6 aerosol particle number concentrations are on average 3-4 higher than the
7 Antarctic aerosol annual winter average concentration (121-179 cm⁻³). Our
8 study strongly suggests that new particle formation may have at least two
9 contrasting sources. The former is related to sea ice marginal zones formed in
10 the marine boundary layer. The latter is related to air masses arriving from the
11 Antarctic plateau, possibly having a free troposphere origin.

12 The biogenic precursors responsible for the new particle formation are not
13 known. Charlson et al. (1987) postulated the CLAW hypothesis - the most
14 significant source of CCN in the marine environment is non-sea-salt sulfate
15 derived from atmospheric oxidation of dimethylsulfide (DMS); however
16 measurements able to provide information on where individual particles come
17 from are still limited (O'Dowd et al., 1997b; Quinn and Bates, 2011; Sanchez
18 et al., 2018). A previous ship-borne field campaign in the Weddell Sea found
19 increased new particle formation in the sea ice zone of the Weddell Sea
20 (Davison et al., 1996), but no clear correlation to the dimethyl sulphide that
21 was then assumed to control new particle bursts. A smaller mode radius
22 associated with polar aerosol (relative to marine Southern ocean aerosol) was
23 found associated with less cloud cover, and consequently less cloud
24 processing, over the continent and pack ice regions. During the cruise, new
25 particle formation observed over the Weddell Sea, resulted from boundary
26 layer nucleation bursts rather than tropospheric entrainment. Brooks and
27 Thornton (2018) argued that additional modeling studies are still needed that
28 address contributions from both secondary DMS-derived aerosols and primary
29 organic aerosols as CCNs on realistic timescales; although the occurrence of
30 a "seasonal CLAW" in remote marine atmospheres is becoming plausible
31 (Vallina and Simó, 2007; Quinn et al., 2017; Sanchez et al., 2018).

32
33 Satellite (Schonhardt et al., 2008) and on-site measurements (Saiz-Lopez et
34 al., 2007; Atkinson et al., 2012) showed that the Weddell Sea is an iodine

Eliminado: baseline

Eliminado: .

1 hotspot; however there was no short-term correlation between IO and particle
2 concentration found (Roscoe et al., 2015). Using an unprecedented suite of
3 instruments, Jokinen et al. (2018) showed that ion-induced nucleation of
4 sulfuric acid and ammonia, followed by sulfuric acid-driven growth, is the
5 predominant mechanism for NPF and growth in eastern Antarctica a few
6 hundred kilometers from the coast (Finnish Antarctic research station (Aboa)
7 is located at the Queen Maud land, Eastern Antarctica; Jokinen et al., 2018).
8 Some ion clusters contained iodic acid, but its concentration was very small,
9 and no pure iodic acid or iodine oxide clusters were detected (Sipila et al.,
10 2016). Finally, some organic oxidation products from land melt ponds have
11 also been suggested (Kyro et al., 2013) as a potential source for condensable
12 vapor, although this may be a confined and minor source (Weller et al., 2018).
13 Other measurements of new particle formation and growth were governed by
14 the availability of other yet unidentified gaseous precursors, most probably low
15 volatile organic compounds of marine origin (Weller et al., 2015; 2018).

16

17 **4.2 Implication for climate and conclusion**

18

19 A strong annual cycle of total particle number concentration is a prominent
20 characteristic of the Antarctic aerosol system, with the austral summer
21 concentration being up to 20-100 times greater than during the winter (Shaw
22 1988, Gras 1993, Ito 1993, Hara et al 2011, Weller et al 2011, Järvinen et al
23 2013, Fiebig et al 2014, Kim et al 2017). These summer particle number
24 concentration maxima are largely explained by NPF taking place in the
25 Antarctic atmosphere. However, these seasonal cycles are more pronounced
26 at monitoring sites situated on the upper plateau of Antarctica than at the
27 coastal Antarctic sites. It is worth to keep in mind that these cycles could also
28 be more pronounced because in coastal regions in winter, sea salt aerosol
29 has a relatively larger source. i.e. the amplitude of the seasonal is driven both
30 by what is going on in winter as well as summer. Nevertheless, overall much
31 higher particle number concentrations have long been reported in coastal
32 Antarctica relative to the plateau. The vertical location of Antarctic NPF has
33 not been well quantified; there are some indications that NPF takes place

1 preferentially in the Antarctic Free Troposphere (FT) rather than in the
2 Boundary Layer (BL) (Koponen et al 2002, Hara et al 2011, Humphries et al
3 2016), whereas other studies shows opposite trends (Kim et al., 2017, Weller
4 et al., 2011; 2013; 2018). A study conducted on the upper plateau of
5 Antarctica demonstrates that also wintertime regional NPF is possible in this
6 environment (Järvinen et al 2013). Very low particle growth rates (between
7 about 0.1 and 1 nm h⁻¹) were reported in Antarctica (Park et al 2004, Weller et
8 al 2015).

9

10 We obtained data from Dome C and King Sejong (KS) Station for the period
11 May-December 2015, and compared them with Halley (H). Data are shown in
12 Fig. 6 where seasonal mean aerosol size distributions measured
13 simultaneously at three different sites are reported for (a) May-December
14 2015 (8 months in total); (b) Spring (September, October, November, 3
15 months in total); (c) Summer (December, 1 month in total) and (d) Winter
16 (June, July, August, 3 months in total, a map of the three stations considered
17 is shown in Figure 7. Overall, much higher concentrations are seen at the
18 coastal Antarctic sites (H, KS stations) relative to Dome C station (Fig. 6a).

19 The presence of permanent Antarctic stations could also affect aerosol size
20 distributions (Kim et al., 2017), future studies will aim at comparing aerosol
21 size distributions data simultaneously collected in different Antarctic stations.

22 Two broad modes at about 30-50 nm and at about 110-160 nm can be seen
23 for the coastal stations, whereas a smaller single mode at 60 nm is seen for
24 the Dome C station. When three seasons are compared, very different
25 features can be seen. During spring (Fig. 6b), both Aitken and accumulation
26 modes dominate the coastal sites, whereas a strong single mode is seen in
27 the Dome C site. By contrast, during summer (Fig. 6c), much stronger
28 nucleation and Aitken modes are seen at the coastal sites, likely due to NPF
29 taking place during summer time. The smaller nucleation mode size detected
30 in the Antarctic peninsula (King Sejong Station) relative to the one seen at
31 Halley may suggest a more local source of NPF in the Antarctic peninsula,
32 including open water, coastal macroalgae, and bird colonies. The average
33 size distributions during winter (Fig. 6d) again show marked differences
34 among the three different monitoring sites. Halley stations shows the largest

1 aerosol modes (about 100 nm and 160 nm), whereas smaller modes can be
2 seen at the other two sites. Overall, Fig. 6 serves to stress that the aerosol
3 population in Antarctica - an environment often considered homogenous and
4 simple to study - is different in different geographical regions, and very likely a
5 number of different processes and sources affect the aerosol population at
6 different times of the year. Ito et al. (1993) presented a conceptual diagram,
7 where different aerosol size distributions were seen, and a main NPF mode
8 was associated with the free troposphere and transported by katabatic winds.
9 Korhonen et al. (2008) also estimated that over 90% of the non-sea spray
10 CCN were generated above the boundary layer by nucleation of sulfuric acid
11 aerosol in the free troposphere. Our results point to sea ice regions and open
12 ocean water being a source not only of gaseous precursors, but also of new
13 particle formation, which then can growth once lifted in the free troposphere
14 (Fig. 8), and then larger modes are brought down again by the Antarctic
15 Drainage flow (James, 1989). The relative importance of free troposphere
16 versus boundary layer nucleation is not known at this stage, but this study
17 shows that the latter is seen, and the former is likely to happen and contribute
18 to the Aitken mode detected from the Antarctic plateau. Sea ice regions
19 (mainly via secondary processes, but also to a lesser degree via sea spray
20 and blowing snow) may control the CCN production, both regulating the first
21 stage of nucleation events and providing gaseous precursors, and slowly
22 growing nucleated particles with transport in the upper troposphere.

23
24 These results are in line with previous studies in polar areas. First, Dall'Osto
25 et al (2017) suggested that the microbiota of sea ice and sea ice-influenced
26 ocean were a significant source of atmospheric nucleating particles
27 concentrations (N_{1-3nm}). Second, within two different Arctic locations, across
28 large temporal scales (2000-2016) new particle formation was associated with
29 air mass back trajectories passing over open water and melting sea ice
30 regions, also pointing to marine biological activities within the open leads in
31 the pack ice and/or along the melting marginal sea ice zone (MIZ) being
32 responsible for such events (Dall'Osto et al., 2017b, Dall'Osto et al., 2018).
33 Our data from Halley, and the brief intercomparison with two other stations,
34 suggest that the size distributions of Antarctic submicron aerosols may have

Con formato: Interlineado:
1,5 líneas

1 been oversimplified in the past (Ito et al., 1993); and complex interactions
2 between multiple ecosystems, coupled with different atmospheric circulation,
3 result in very different aerosol size distributions populating the Southern
4 Hemisphere. We simply know too little about the sources of primary and
5 secondary aerosols of biogenic origin. Further studies are needed in order to
6 quantify the baseline aerosol properties in the polar regions and how they are
7 affected by emission processes and atmospheric processing and aging.
8 Future work in preparation will soon address these questions by an analysis of
9 aerosol size distributions simultaneously detected around the Antarctic
10 continent.

Eliminado: ¶
¶

11
12 Data availability. Data can be accessed by contacting the corresponding
13 author.

Con formato: Fuente: Cursiva

14
15 Supplement. The supplement related to this article is available online.

Con formato: Fuente: Cursiva

16
17 Author contributions. DB and MD conducted the analysis and wrote the
18 manuscript. TCL, NB and AJ provided the Halley SMPS data. AL, YJY, AV
19 provided additional SMPS data. All authors edited and contributed to
20 subsequent drafts of the manuscript.

Con formato: Fuente: Cursiva

Con formato: Interlineado:
1,5 líneas

21
22 Competing interests. The authors declare that they have no conflicts of
23 interest.

Con formato: Fuente: Cursiva

24
25 Financial support. The study was further supported by the Spanish Ministry of
26 Economy through project PI-ICE (CTM 2017–89117-R) and the Ramon y
27 Cajal fellowship (RYC-2012-11922). The National Centre for Atmospheric
28 Science NCAS Birmingham group is funded by the UK Natural Environment
29 Research Council. AV was supported by the Academy of Finland's Centre of
30 Excellence program (Centre of Excellence in Atmospheric Science – From
31 Molecular and Biological processes to The Global Climate, project no.
32 272041). KS station SMPS measurement was supported by KOPRI project
33 (PE19010).

Con formato: Fuente: Cursiva

1 ~~*Acknowledgements.*~~ The authors are grateful to the overwintering staff at
2 Halley station who carried out the suite of measurements presented here. This
3 work was funded by the Natural Environment Research Council as part of the
4 British Antarctic Survey's research programme "Polar Science for Planet
5 Earth". ~~We thank~~ We thank Dr. Pasi Aalto (Institute for Atmospheric and Earth
6 System Research, University of Helsinki) and the joint French-Italian
7 Concordia Program with the project LTCPAA, for providing DMPS data of
8 2015 for intercomparison with data taken at Halley Station, similar data were
9 discussed in details elsewhere (Järvinen et al., 2013; Kim et al., 2017) .

10
11 *Review statement.* This paper was edited by Veli-Matti Kerminen and
12 reviewed by three anonymous referees.

13 14 15 16 17 18 **References**

19
20
21 Asmi, E., Frey, A., Virkkula, A., Ehn, M., Manninen, H., Timonen, H., Tolonen-
22 Kivimäki, O., Aurela, M., Hillamo, R., and Kulmala, M.: Hygroscopicity and
23 chemical composition of Antarctic sub-micrometre aerosol particles and
24 observations of new particle formation, *Atmos. Chem. Phys.*, 10, 4253–4271,
25 <https://doi.org/10.5194/acp-10-4253-2010>, 2010.

26
27
28 Atkinson, H. M., R.-J. Huang, R. Chance, H. K. Roscoe, C. Hughes, B. Avison,
29 A. Schönhardt, A. S. Mahajan, A. Saiz-Lopez, and P. S. Liss (2012), Iodine
30 emissions from the sea ice of the Weddell Sea, *Atmos. Chem. Phys.*, 12,
31 11,229–11,244, doi:10.5194/acp-12-11229-2012.

32
33 Becagli, S., Scarchilli, C., Traversi, R., Dayan, U., Severi, M., Frosini, D.,
34 Vitale, V., Mazzola, M., Lupi, A., Nava, S., and Udisti, R.: Study of present-day
35 sources and transport processes affecting oxidised sulphur compounds in
36 atmospheric aerosols at Dome C (Antarctica) from year-round sampling
37 campaigns, *Atmos. Environ.*, 52, 98–108,
38 <https://doi.org/10.1016/j.atmosenv.2011.07.053>, 2012.

39
40 Beddows, D. C. S., Dall'Osto, M., and Harrison, R. M.: Cluster Analysis of
41 Rural, Urban and Curbside Atmospheric Particle Size Data, *Environ. Sci.*
42 *Technol.*, 43, 4694–4700, 2009.

Eliminado: ¶

Con formato: Fuente: Sin
Negrita, Cursiva

Eliminado: ¶

Eliminado: The study was further supported by the Spanish Ministry of Economy through project PI-ICE (CTM 2017-89117-R) and the Ramon y Cajal fellowship (RYC-2012-11922). The National Centre for Atmospheric Science NCAS Birmingham group is funded by the UK Natural Environment Research Council.

Eliminado: Dr. Pasi aalto (Institute for Atmospheric and Earth System Research, University of Helsinki)

Eliminado: AV as supported by the Academy of Finland's Centre of Excellence program (Centre of Excellence in Atmospheric Science – From Molecular and Biological processes to The Global Climate, project no. 272041). KS station SMPS measurement was supported by KOPRI project (PE19010).¶

Eliminado: ¶

1 Beddows, D. C. S., Dall’Osto, M., Harrison, R. M., Kulmala, M., Asmi, A.,
2 Wiedensohler, A., Laj, P., Fjaeraa, A. M., Sellegri, K., Birmili, W., Bukowiecki,
3 N., Weingartner, E., Baltensperger, U., Zdimal, V., Zikova, N., Putaud, J.-P.,
4 Marinoni, A., Tunved, P., Hansson, H.-C., Fiebig, M., Kivekäs, N., Swietlicki, E.,
5 Lihavainen, H., Asmi, E., Ulevicius, V., Aalto, P. P., Mihalopoulos, N., Kalivitis,
6 N., Kalapov, I., Kiss, G., de Leeuw, G., Henzing, B., O’Dowd, C., Jennings, S.
7 G., Flentje, H., Meinhardt, F., Ries, L., Denier van der Gon, H. A. C., and
8 Visschedijk, A. J. H.: Variations in tropospheric submicron particle size
9 distributions across the European continent 2008–2009, *Atmos. Chem. Phys.*,
10 14, 4327–4348, <https://doi.org/10.5194/acp-14-4327-2014>, 2014.

11
12 [Beddows, D. C. S. and Harrison, R. M.: Receptor modelling of both particle
13 composition and size distribution from a background site in London, UK – a
14 two-step approach, *Atmos. Chem. Phys.*, 19, 4863–4876,
15 <https://doi.org/10.5194/acp-19-4863-2019>, 2019.](https://doi.org/10.5194/acp-19-4863-2019)

16
17 Bertram, T.H.; Cochran, R.E.; Grassian, V.H.; Stone, E.A. Sea spray aerosol
18 chemical composition: Elemental and molecular mimics for laboratory studies
19 of heterogeneous and multiphase reactions. *Chem. Soc. Rev.*
20 2018, 47, 2374–2400

21
22 Boucher, O., Randall, D., Artaxo, P., Bretherton, C., Feingold, G., Forster, P.,
23 Kerminen, V. M., Kondo, Y., Liao, H., Lohmann, U., Rasch, P., Satheesh, S.,
24 Sherwood, S., Stevens, B., and Zhang, X.: Clouds and aerosols, in: *Climate
25 change 2013: the physical science basis. Contribution of working group I to
26 the fifth assessment report of the intergovernmental panel on climate change*,
27 edited by: Stocker, T. F., Qin, D., Plattner, G. K., Tignor, M., Allen, S.,
28 Boschung, J., Nauels, A., Xia, Y., Bex, V., and Midgley, P., chap. 7,
29 Cambridge University Press, Cambridge, 2013.

30
31 Brooks, S. D. and Thornton, D. C. O.: Marine Aerosols and Clouds,
32 *Annu. Rev. Mar. Sci.*, 10, 289–313, 2018

33
34 Carslaw, K. S., Lee, L. A., Reddington, C. L., Pringle, K. J., Rap, A., Forster, P.
35 M., Mann, G.W., Spracklen, D. V., Woodhouse, M. T., Regayre, L. A., and
36 Pierce, J. R.: Large contribution of natural aerosols to uncertainty in indirect
37 forcing,

38
39 Carslaw, D. C. and K. Ropkins, (2012) openair --- an R package for air quality
40 data analysis. *Environmental Modelling & Software*. Volume 27-28, 52-61.
41 10.1016/j.envsoft.2011.09.008

42
43 Charlson, R. J., Lovelock, J. E., Andreae, M. O., and Warren, S. G.: Oceanic
44 Phytoplankton, Atmospheric Sulfur, Cloud Albedo and Climate, *Nature*, 326,
45 655–661, <https://doi.org/10.1038/326655a0>, 1987.

46
47 Chen, J. L., C. R. Wilson, D. Blankenship, and B. D. Tapley
48 (2009), Accelerated Antarctic ice loss from satellite gravity
49 measurements, *Nat. Geosci.*, 2, 859–862, doi:10.1038/ngeo694.

50

1 Dall'Osto, M., Monahan, C., Greaney, R., Beddows, D. C. S., Harrison, R. M.,
2 Ceburnis, D., and O'Dowd, C. D.: A statistical analysis of North East Atlantic
3 (submicron) aerosol size distributions, *Atmos. Chem. Phys.*, 11, 12567–12578,
4 <https://doi.org/10.5194/acp-11-12567-2011>, 2011.

5
6 Dall'Osto, M., Beddows, D. C. S., Tunved, P., Krejci, R., Ström, J., Hansson,
7 H.-C., Yoon, Y. J., Park, K.-T., Becagli, S., Udisti, R., Onasch, T., O'Dowd, C.
8 D., Simó, R., and Harrison, R. M.: Arctic sea ice melt leads to atmospheric new
9 particle formation, *Sci. Rep.*, 7, 3318, [https://doi.org/10.1038/s41598-017-](https://doi.org/10.1038/s41598-017-03328-1)
10 [03328-1](https://doi.org/10.1038/s41598-017-03328-1), 2017a

11
12 Dall'Osto, M., Ovadnevaite, J., Paglione, M., Beddows, D. C. S., Ceburnis, D.,
13 Cree, C., Cortes, P., Zamanillo, M., Nunes, S. O., Perez, G. L., Ortega-
14 Retuerta, E., Emelianov, M., Vaque, D., Marrase, C., Estrada, M., Sala, M. M.,
15 Vidal, M., Fitzsimons, M. F., Beale, R., Ayr, R., Rinaldi, M., Decesari, S.,
16 Facchini, M. C., Harrison, R. M., O'Dowd, C., and Simo, R.: Antarctic sea
17 ice region as a source of biogenic organic nitrogen in aerosols, *Scientific*
18 *Reports*, 7, 6047, [https://doi.org/10.1038/s41598-017-](https://doi.org/10.1038/s41598-017-06188-x)
19 [06188-x](https://doi.org/10.1038/s41598-017-06188-x), 2017b

20
21
22 Dall'Osto, M., Beddows, D. C. S., Asmi, A., Poulain, L., Hao, L., Freney, E.,
23 Allan, J. D., Canagaratna, M., Crippa, M., Bianchi, F., de Leeuw, G., Eriksson,
24 A., Swietlicki, E., Hansson, H. C., Henzing, J. S., Granier, C., Zemann, K.,
25 Laj, P., Onasch, T., Prevot, A., Putaud, J. P., Sellegri, K., Vidal, M., Virtanen,
26 A., Simo, R., Worsnop, D., O'Dowd, C., Kulmala, M., and Harrison, R. M.:
27 Novel insights on new particle formation derived from a paneuropean
28 observing system, *Sci. Rep.*, 8, 1482, [https://doi.org/10.1038/s41598-017-](https://doi.org/10.1038/s41598-017-17343-9)
29 [17343-9](https://doi.org/10.1038/s41598-017-17343-9), 2018a.

30
31 Dall'Osto, M., Geels, C., Beddows, D. C. S., Boertmann, D., Lange, R.,
32 Nøjgaard, J. K., Harrison Roy, M., Simo, R., Skov, H., Massling, A. Regions of
33 open water and melting sea ice drive new particle formation in North East
34 Greenland. *Sci. Rep.* 8, 6109., 2018b

35
36 Dall'Osto, M., Beddows, D. C. S., Tunved, P., Harrison, R. M., Lupi, A., Vitale,
37 V., Becagli, S., Traversi, R., Park, K.-T., Yoon, Y. J., Massling, A., Skov, H.,
38 Lange, R., Strom, J., and Krejci, R.: Simultaneous measurements of aerosol
39 size distributions at three sites in the European high Arctic, *Atmos. Chem.*
40 *Phys.*, 19, 7377–7395, <https://doi.org/10.5194/acp-19-7377-2019>, 2019.

41
42
43 Davison, B., O'Dowd, C., Hewitt, C., Smith, M., Harrison Roy, M., Peel, D., Wolf, E.,
44 Mulvaney, R., Schwikowski, M., and Baltensperger, U.: Dimethylsulfide and its
45 oxidation products in the atmosphere of the Atlantic and southern oceans,
46 *Atmos. Environ.*, 30, 1895–1906, 1996.

47
48 Doug McIlroy. Packaged for R by Ray Brownrigg, Thomas P Minka and
49 transition to Plan 9 codebase by Roger Bivand. (2018). mapproj: Map

1 Projections. R package version 1.2.6. [https://CRAN.R-](https://CRAN.R-project.org/package=mapproj)
2 [project.org/package=mapproj](https://CRAN.R-project.org/package=mapproj)
3
4 Fiebig, M., Hirdman, D., Lunder, C. R., Ogren, J. A., Solberg, S., Stohl, A.,
5 and Thompson, R. L.: Annual cycle of Antarctic baseline aerosol: controlled by
6 photooxidation-limited aerosol formation, *Atmos. Chem. Phys.*, 14, 3083-3093,
7 <https://doi.org/10.5194/acp-14-3083-2014>, 2014.
8
9 Frey, M. M., Norris, S. J., Brooks, I. M., Anderson, P. S., Nishimura, K., Yang,
10 X., Jones, A. E., Nerentorp Mastromonaco, M. G., Jones, D. H., and Wolff, E.
11 W.: First direct observation of sea salt aerosol production from blowing snow
12 above sea ice, *Atmos. Chem. Phys. Discuss.*, [https://doi.org/10.5194/acp-](https://doi.org/10.5194/acp-2019-259)
13 [2019-259](https://doi.org/10.5194/acp-2019-259), in review, 2019.
14
15 Fossum, K. N., Ovadnevaite, J., Ceburnis, D., Dall'Osto, M., Marullo, S.,
16 Bellacicco, M., Simó, R., Liu, D., Flynn, M., Zuend, A., O'Dowd, C.:
17 Summertime primary and secondary contributions to Southern Ocean cloud
18 condensation nuclei, *Scientific Reports.*, 8, 13844, 2018.
19
20 Galí, M., Levasseur, M., Devred, E., Simó, R., and Babin, M.: Sea-surface
21 dimethylsulfide (DMS) concentration from satellite data at global and regional
22 scales, *Biogeosciences*, 15, 3497-3519, [https://doi.org/10.5194/bg-15-3497-](https://doi.org/10.5194/bg-15-3497-2018)
23 [2018](https://doi.org/10.5194/bg-15-3497-2018), 2018.
24
25 Gantt, B. and Meskhidze, N.: The physical and chemical characteristics of
26 marine primary organic aerosol: a review, *Atmos. Chem. Phys.*, 13, 3979–
27 3996, [doi:10.5194/acp-13-3979-2013](https://doi.org/10.5194/acp-13-3979-2013), 2013.
28
29 Giordano, M. R., Kalnajs, L. E., Avery, A., Goetz, J. D., Davis, S. M., and
30 DeCarlo, P. F.: A missing source of aerosols in Antarctica – beyond long-
31 range transport, phytoplankton, and photochemistry, *Atmos. Chem. Phys.*, 17,
32 1–20, [https://doi.org/10.5194/acp-](https://doi.org/10.5194/acp-17-1-2017)
33 [17-1-2017](https://doi.org/10.5194/acp-17-1-2017), 2017
34
35 Giordano, M. R., Kalnajs, L. E., Goetz, J. D., Avery, A. M., Katz, E., May, N.
36 W., Leemon, A., Mattson, C., Pratt, K. A., and DeCarlo, P. F.: The importance
37 of blowing snow to halogen-containing aerosol in coastal Antarctica: influence
38 of source region versus wind speed, *Atmos. Chem. Phys.*, 18, 16689–16711,
39 <https://doi.org/10.5194/acp-18-16689-2018>, 2018.
40
41 Gras, J. L. and Keywood, M.: Cloud condensation nuclei over the Southern
42 Ocean: wind dependence and seasonal cycles, *Atmos. Chem. Phys.*, 17,
43 4419–4432, <https://doi.org/10.5194/acp-17-4419-2017>, 2017.
44
45 [Halkidi, M., Batistakis, Y., Vazirgiannis, M., \(2001\) On Clustering Validation](#)
46 [Techniques, Journal of Intelligent Information Systems, 17:2/3, 107–145.](#)
47
48 Hamed, A., Korhonen, H., Sihto, S.-L., Joutsensaari, J., Jarvinen, H., Petaja,
49 T., Arnold, F., Nieminen, T., Kulmala, M., Smith, J. N., Lehtinen, K. E. J., and

1 Laaksonen, A.: The role of relative humidity in continental new particle
2 formation, *J. Geophys. Res.*, 116, D03202, doi:10.1029/2010JD014186, 2011.
3
4 Hamilton, D. S., L. A. Lee, K. J. Pringle, C. L. Reddington, D. V. Spracklen,
5 and K. S. Carslaw, Occurrence of pristine aerosol environments on a polluted
6 planet, *P Natl Acad Sci USA*, 111, 18466–18471,
7 doi:10.1073/pnas.1415440111, 2014
8
9 Hara K, Osada K, Nishita-Hara Cand Yamanouchi T 2011 Seasonal variations
10 and vertical features of aerosol particles in the Antarctic troposphere *Atmos.*
11 *Chem. Phys.* 11 5471–84
12
13 Herenz, P., Wex, H., Mangold, A., Laffineur, Q., Gorodetskaya, I. V., Fleming,
14 Z. L., Panagi, M., and Stratmann, F.: CCN measurements at the Princess
15 Elisabeth Antarctica research station during three austral summers, *Atmos.*
16 *Chem. Phys.*, 19, 275–294, <https://doi.org/10.5194/acp-19-275-2019>, 2019.
17
18 Hodshire A L et al 2016 Multiple new-particle growth pathways observed at
19 the USDOESouthern Great Plains field site *Atmos. Chem. Phys.* 16 9321–48
20
21 Hoppel, W.A., Frick, G.M., Fitzgerald, J.W., 1994. Marine boundary layer
22 measurements of new-particle formation and the effects of non-precipitating
23 clouds have on aerosol size distribution. *J. Geophys. Res.* 99, 14443–14459
24
25 Humphries, R. S., Schofield, R., Keywood, M. D., Ward, J., Pierce, J. R.,
26 Gionfriddo, C. M., Tate, M. T., Krabbenhoft, D. P., Galbally, I. E., Molloy, S. B.,
27 Klekociuk, A. R., Johnston, P. V., Kreher, K., Thomas, A. J., Robinson, A. D.,
28 Harris, N. R. P., Johnson, R., and Wilson, S. R.: Boundary layer new particle
29 formation over East Antarctic sea ice – possible Hg-driven nucleation?, *Atmos.*
30 *Chem. Phys.*, 15, 13339–13364, <https://doi.org/10.5194/acp-15-13339-2015>,
31 2015.
32
33 Huang, J., Jaeglé, L., and Shah, V.: Using CALIOP to constrain blowing snow
34 emissions of sea salt aerosols over Arctic and Antarctic sea ice, *Atmos. Chem.*
35 *Phys.*, 18, 16253–16269, <https://doi.org/10.5194/acp-18-16253-2018>, 2018.
36
37
38 Ito T 1993 Size distribution of Antarctic submicron aerosols *Tellus B*
39 45 145–59
40
41 Jang, E., Park, K.-T., Yoon, Y. J., Kim, T.-W., Hong, S.-B., Becagli, S., raversi,
42 R., Kim, J., and Gim, Y.: New particle formation events observed at the King
43 Sejong Station, Antarctic Peninsula – Part 2: Link with the oceanic biological
44 activities, *Atmos. Chem. Phys.*, 19, 7595–7608, [https://doi.org/10.5194/acp-](https://doi.org/10.5194/acp-19-7595-2019)
45 [19-7595-2019](https://doi.org/10.5194/acp-19-7595-2019), 2019.
46
47 Järvinen, E., Virkkula, A., Nieminen, T., Aalto, P. P., Asmi, E., Lanconelli,
48 C., Busetto, M., Lupi, A., Schioppo, R., Vitale, V., Mazzola, M., Petäjä, T.,
49 Kerminen, V.-M., and Kulmala, M.: Seasonal cycle and modal structure of

1 particle number size distribution at Dome C, Antarctica, Atmos. Chem. Phys.,
2 13, 7473–7487, <https://doi.org/10.5194/acp-13-7473-2013>, 2013.

3
4 Jokinen, T., Sipilä, M., Kontkanen, J., Vakkari, V., Tisler, P., Duplissy, E.-M.,
5 Junninen, H., Kangasluoma, J., Manninen, H. E., Petäjä, T., Kulmala,
6 M., Worsnop, D. R., Kirkby, J., Virkkula, A., and Kerminen, V.-M.: Ion-induced
7 sulfuric acid–ammonia nucleation drives particle formation in coastal
8 Antarctica, Sci. Adv., 4, eaat9744, <https://doi.org/10.1126/sciadv.aat9744>,
9 2018.

10
11 [Jones, A. E., Wolff, E. W., Salmon, R. A., Bauguitte, S. J.-B., Roscoe, H. K.,](#)
12 [Anderson, P. S., Ames, D., Clemitshaw, K. C., Fleming, Z. L., Bloss, W. J.,](#)
13 [Heard, D. E., Lee, J. D., Read, K. A., Hamer, P., Shallcross, D. E., Jackson, A.](#)
14 [V., Walker, S. L., Lewis, A. C., Mills, G. P., Plane, J. M. C., Saiz-Lopez, A.,](#)
15 [Sturges, W. T., and Worton, D. R.: Chemistry of the Antarctic Boundary Layer](#)
16 [and the Interface with Snow: an overview of the CHABLIS campaign, Atmos.](#)
17 [Chem. Phys., 8, 3789–3803, https://doi.org/10.5194/acp-8-3789-2008, 2008.](#)

18
19 Jung, J., Hong, S.-B., Chen, M., Hur, J., Jiao, L., Lee, Y., Park, K., Hahm, D.,
20 Choi, J.-O., Yang, E. J., Park, J., Kim, T.-W., and Lee, S.: Characteristics of
21 biogenically-derived aerosols over the Amundsen Sea, Antarctica, Atmos.
22 Chem. Phys. Discuss., <https://doi.org/10.5194/acp-2019-133>, in review, 2019.

23
24 Kalnay E., M. Kanamitsu, R. Kistler, W. Collins, D. Deaven, L. Gandin, M.
25 Iredell, S. Saha, G. White, J. Woollen, Y. Zhu, M. Chelliah, W. Ebisuzaki, W.
26 Higgins, J. Janowiak, K.C. Mo, C. Ropelewski, J. Wang, A. Leetmaa, R.
27 Reynolds, R. Jenne, D. Joseph The NCEP/NCAR 40-year Reanalysis project
28 Bull. Am. Met. Soc., 77, pp. 437-471. <http://dx.doi.org/10.1175/1520->
29 [0477\(1996\)077<0437:TNYRP>2.0.CO;2](http://dx.doi.org/10.1175/1520-0477(1996)077<0437:TNYRP>2.0.CO;2), 1996

30
31 Kerminen, V.-M., Chen, X., Vakkari, V., Petäjä, T., Kulmala, M., and Bianchi,
32 F.: Atmospheric new particle formation and growth: review of field observations,
33 Environ. Res. Lett., 13, 103003, <https://doi.org/10.1088/1748-9326/aadf3c>,
34 2018.

35
36 Kim, J., Yoon, Y. J., Gim, Y., Kang, H. J., Choi, J. H., Park, K.-T., and Lee, B.
37 Y.: Seasonal variations in physical characteristics of aerosol particles at the
38 King Sejong Station, Antarctic Peninsula, Atmos. Chem. Phys., 17, 12985–
39 12999, <https://doi.org/10.5194/acp-17-12985-2017>, 2017.

40
41 [Kim, J., Yoon, Y. J., Gim, Y., Choi, J. H., Kang, H. J., Park, K.-T., Park, J., and](#)
42 [Lee, B. Y.: New particle formation events observed at King Sejong Station,](#)
43 [Antarctic Peninsula – Part 1: Physical characteristics and contribution to cloud](#)
44 [condensation nuclei, Atmos. Chem. Phys., 19, 7583–7594,](#)
45 <https://doi.org/10.5194/acp-19-7583-2019>, 2019.

46
47 Koponen IK, Virkkula A, Hillamo R, Kerminen V-M and Kulmala M. Number
48 size distributions of marine aerosols: observations during a cruise between
49 the English Channel and coast of Antarctica J. Geophys. Res. 107 4753, 2002

Eliminado: ¶

1 Koponen IK, Virkkula A, Hillamo R, Kerminen V-M and Kulmala M Number size
2 distributions and concentrations of the continental summer aerosols in Queen
3 Maud Land, Antarctica J. Geophys. Res. 108 4587, 2003
4
5 Korhonen, H., Carslaw, K. S., Spracklen, D. V., Mann, G., W., and Woodhouse,
6 M. T.: Influence of oceanic dimethyl sulfide emissions on cloud condensation
7 nuclei concentrations and seasonality over the remote Southern Hemisphere
8 oceans: A global model study, J. Geophys. Res.-Atmos., 113, D15204,
9 doi:10.1029/2007JD009718, 2008
10
11 Laaksonen, A., Kulmala, M., O'Dowd, C. D., Joutsensaari, J., Vaattovaara, P.,
12 Mikkonen, S., Lehtinen, K. E. J., Sogacheva, L., DalMaso, M., Aalto, P.,
13 Petäjä, T., Sogachev, A., Yoon, Y. J., Lihavainen, H., Nilsson, D., Facchini, M.
14 C., Cavalli, F., Fuzzi, S., Hoffmann, T., Arnold, F., Hanke, M., Sellegri, K.,
15 Umann, B., Junkermann, W., Coe, H., Allan, J. D., Alfarra, M. R., Worsnop,
16 D. R., Riekkola, M. -L., Hyötyläinen, T., and Viisanen, Y.: The role of VOC
17 oxidation products in continental new particle formation, Atmos. Chem. Phys.,
18 8, 2657–2665, doi:10.5194/acp-8-2657-2008, 2009
19
20 [Lange, R., Dall'Osto, M., Skov, H., Nielsen, I. E., David Beddows, Simo, R.,](#)
21 [Roy Harrison & Massling, A., 29 Mar 2018, Characterization of distinct Arctic](#)
22 [Aerosol Accumulation Modes and their Sources, Atmospheric Environment,](#)
23 [183, p. 1-10](#)
24
25 Liu, J., Dedrick, J., Russell, L. M., Senum, G. I., Uin, J., Kuang, C., Springston,
26 S. R., Leaitch, W. R., Aiken, A. C., and Lubin, D.: High summertime aerosol
27 organic functional group concentrations from marine and seabird sources at
28 Ross Island, Antarctica, during AWARE, Atmos. Chem. Phys., 18, 8571–8587,
29 <https://doi.org/10.5194/acp-18-8571-2018>, 2018.
30
31 McCoy, D. T., Burrows, S. M., Wood, R., Grosvenor, D. P., Elliott, S. M., Ma,
32 P.-L., Rasch, P. J., and Hartmann, D.L.: Natural aerosols explain seasonal
33 and spatial patterns of Southern Ocean cloud albedo, Sci. Adv., 1, e1500157,
34 <https://doi.org/10.1126/sciadv.1500157>, 2015
35
36 Murphy, D. M., Froyd, K. D., Bian, H., Brock, C. A., Dibb, J. E., DiGangi, J.
37 P., Diskin, G., Dollner, M., Kupc, A., Scheuer, E. M., Schill, G. P., Weinzierl, B.,
38 Williamson, C. J., and Yu, P.: The distribution of sea-salt aerosol in the global
39 troposphere, Atmos. Chem. Phys., 19, 4093-4104,
40 <https://doi.org/10.5194/acp-19-4093-2019>, 2019.
41
42 O'Dowd, C.D., Smith, M.H., Consterdine, I.E., Lowe, J.A., 1997a. Marine
43 aerosol, sea-salt, and the marine sulphur cycle—a short review. Atmos. Environ.
44 31, 73–80, 1997a
45
46 O'Dowd, CO, J. A. Lowe, M. H. Smith, B. Davison, C. N. Hewitt, R. M.
47 Harrison, Biogenic sulphur emissions and inferred non-sea-salt-sulphate cloud
48 condensation nuclei in and around Antarctica. J. Geophys. Res. Atmos. 102,
49 12839–12854, 1997b
50

1 Quinn, P. K. and Bates, T. S.: The case against climate regulation via oceanic
2 phytoplankton sulphur emissions, *Nature*,480(7375), 51–56,
3 doi:10.1038/nature10580, 2011
4
5 Quinn, P. K., Collins, D. B., Grassian, V. H., Prather, K. A.,and Bates, T. S.:
6 Chemistry and Related Properties of FreshlyEmitted Sea Spray Aerosol, *hem.*
7 *Rev.*, 115, 4383–4399, doi:10.1021/cr500713g, 2015
8
9 Quinn, P. K., Coffman, D. J., Johnson, J. E., Upchurch, L. M., andBates, T. S.:
10 Small fraction of marine cloud condensation nucleimade up of sea spray
11 aerosol, *Nat. Geosci.*, 10, 674–679,https://doi.org/10.1038/ngeo3003, 2017.
12
13 Rankin, A. M., and E. W. Wolff, A year-long record of size-segregated aerosol
14 composition at Halley, Antarctica,*J. Geophys. Res.*, 108(D24), 4775,
15 doi:10.1029/2003JD003993, 2003.
16
17 Reddington, C., Carslaw, K., Stier, P., Schutgens, N., Coe, H., Liu,D., Allan, J.,
18 Pringle, K., Lee, L., and Yoshioka, M.: The GlobalAerosol Synthesis and
19 Science Project (GASSP): measurements and modelling to reduce uncertainty,
20 *B. Am. Meteorol. Soc.*,98.9, 1857–1877, 2017.
21
22 Richard A. Becker, Allan R. Wilks. R version by Ray Brownrigg.
23 Enhancements by Thomas P Minka and Alex Deckmyn. (2018). maps: Draw
24 Geographical Maps. R package version 3.3.0. [https://CRAN.R-](https://CRAN.R-project.org/package=maps)
25 [project.org/package=maps](https://CRAN.R-project.org/package=maps)
26
27 Robert J. Hijmans (2019). raster: Geographic Data Analysis and Modeling. R
28 package version 2.9-23. <https://CRAN.R-project.org/package=raster>
29
30 Roscoe, H. K., A. E. Jones, N. Brough, R. Weller, A. Saiz-Lopez, A. S.
31 Mahajan, A. Schoenhardt, J. P. Burrows, and Z. L. Fleming (2015), Particles
32 and iodine compounds in coastal Antarctica, *J. Geophys. Res. Atmos.*, 120,
33 7144–7156, doi:10.1002/2015JD023301.
34
35 [Rousseeuw, P..J., \(1987\) Silhouettes: a graphical aid to the interpretation and](#)
36 [validation of cluster analysis, *Journal of Computational and Applied*](#)
37 [*Mathematics* 20, 53-65.](#)
38
39
40 Saiz-Lopez, A., A. S. Mahajan, R. A. Salmon, S. J.-B. Bauguitte, A. E. Jones,
41 H. K. Roscoe, and J. M. C. Plane (2007), Boundary layer halogens in coastal
42 Antarctica, *Science*, 317, 348–351.
43
44 Sanchez, K. J., Chen, C.-L., Russell, L. M., Betha, R., Liu, J., Price, D. J.,
45 Massoli, P., Ziemba, L. D., Crosbie, E. C., Moore, R. H., Müller, M., Schiller, S.
46 A., Wisthaler, A., Lee, A. K. Y., Quinn, P. K., Bates, T. S., Porter, J., Bell, T.
47 G., Saltzman, E. S., Vaillancourt, R. D., and Behrenfeld, M. J.: Substantial
48 seasonal contribution of observed biogenic sulfate particles to cloud
49 condensation nuclei, *Sci. Rep.*, 8, 3235, [https://doi.org/10.1038/s41598-](https://doi.org/10.1038/s41598-018-21590-9)
50 [018-21590-9](https://doi.org/10.1038/s41598-018-21590-9), 2018.

1
2 Schmale, J., Schneider, J., Nemitz, E., Tang, Y. S., Dragosits, U., Blackall, T.
3 D., Trathan, P. N., Phillips, G. J., Sutton, M., and Braban, C. F.: Sub-Antarctic
4 marine aerosol: dominant contributions from biogenic sources, *Atmos. Chem.*
5 *Phys.*, 13, 8669– 8694, <https://doi.org/10.5194/acp-13-8669-2013>, 2013.
6
7 Schönhardt, A., A. Richter, F. Wittrock, H. Kirk, H. Oetjen, H. K. Roscoe, and
8 J. P. Burrows (2008), Observations of iodine monoxide (IO) columns from
9 satellite, *Atmos. Chem. Phys.*, 8, 637–653 Shaw G.E. 1988 Antarctic
10 aerosols: a review *Rev. Geophys.* 26 89–112
11
12 Sipilä, M., Sarnela, N., Jokinen, T., Henschel, H., Junninen, H., Kontkanen, J.,
13 Ichners, S., Kangasluoma, J., Franchin, A., 5 Peräkylä, O., Rissanen, M.P., hn,
14 M., Vehkamäki, H., Kurten, T., Berndt, T., Petäjä, T., Worsnop, D., Ceburnis, .,
15 Kerminen, V.-M., Kulmala, M., O'Dowd, C., 2016. Molecular-scale evidence of
16 aerosol particle formation via sequential addition of HIO₃. *Nature* 537, 532–
17 534. <https://doi.org/10.1038/nature19314>.
18
19 Shaw, G. E.: Considerations on the Origin and Properties of the Antarctic
20 Aerosol, *Rev. Geophys.*, 17, 1983–1998, 1988.
21
22 Teinilä, K., Frey, A., Hillamo, R., Tülp, H. C., and Weller, R.: A study of the
23 sea-salt chemistry using size-segregated aerosol measurements at coastal
24 Antarctic station Neumayer, *Atmos. Environ.*, 96, 11–19, 2014.
25
26 Udisti, R., Dayan, U., Becagli, S., Busetto, M., Frosini, D., Legrand, M.,
27 Lucarelli, F., Preunkert, S., Severi, M., Traversi, R., and Vitale, V.: Sea spray
28 aerosol in central Antarctica. Present atmospheric behaviour and implications
29 for paleoclimatic reconstructions, *Atmos. Environ.*, 52, 109–
30 120, <https://doi.org/10.1016/j.atmosenv.2011.10.018>, 2012.
31
32 Vallina, S. M. and Simó, R.: Re-visiting the CLAW hypothesis, *Environ. Chem.*,
33 4, 384–387, <https://doi.org/10.1071/EN07055>, 2007.
34
35 [Vignon, É., Traullé, O., and Berne, A.: On the fine vertical structure of the low](https://doi.org/10.5194/acp-19-4659-2019)
36 [troposphere over the coastal margins of East Antarctica, *Atmos. Chem. Phys.*,](https://doi.org/10.5194/acp-19-4659-2019)
37 [19, 4659–4683, <https://doi.org/10.5194/acp-19-4659-2019>, 2019.](https://doi.org/10.5194/acp-19-4659-2019)
38
39 Virkkula, A., Teinilä, K., Hillamo, R., Kerminen, V.-M., Saarikoski, S., Aurela,
40 M., Viidanoja, J., Paatero, J., Koponen, I. K., Kulmala, M.: Chemical
41 composition of boundary layer aerosol over the Atlantic Ocean and at an
42 Antarctic site, *Atmos. Chem. Phys.*, 6, 3407–3421, 2006.
43
44 Yang, X., Frey, M. M., Rhodes, R. H., Norris, S. J., Brooks, I. M., Anderson, P.
45 S., Nishimura, K., Jones, A. E., and Wolff, E. W.: Sea salt aerosol production
46 via sublimating wind-blown saline snow particles over sea ice:
47 parameterizations and relevant microphysical mechanisms, *Atmos. Chem.*
48 *Phys.*, 19, 8407–8424, <https://doi.org/10.5194/acp-19-8407-2019>, 2019.
49

1 Weller, R., Minikin, A., Wagenbach, D., and Dreiling, V.: Characterization of
2 the inter-annual, seasonal, and diurnal variations of condensation particle
3 concentrations at Neumayer, Antarctica, *Atmos. Chem. Phys.*, 11, 13243–
4 13257, <https://doi.org/10.5194/acp-11-13243-2011>, 2011.

5
6 Weller, R., Schmidt, K., Teinilä, K., and Hillamo, R.: Natural new particle
7 formation at the coastal Antarctic site Neumayer, *Atmos. Chem. Phys.*, 15,
8 11399–11410, <https://doi.org/10.5194/acp-15-11399-2015>, 2015.

9
10 Weller, R., Legrand, M., and Preunkert, S.: Size distribution and ionic
11 composition of marine summer aerosol at the continental Antarctic site
12 Kohonen, *Atmos. Chem. Phys.*, 18, 2413–2430, <https://doi.org/10.5194/acp-18-2413-2018>, 2018.

14
15 Xu, G. J., Gao, Y., Lin, Q., Li, W., and Chen, L. Q.: Characteristics of water-
16 soluble inorganic and organic ions in aerosols over the Southern Ocean and
17 coastal East Antarctica during austral summer, *J. Geophys. Res.-Atmos.*, 118,
18 13303–13318, <https://doi.org/10.1002/2013jd019496>, 2013.

19
20 Zorn, S. R., Drewnick, F., Schott, M., Hoffmann, T., and Borrmann, S.:
21 characterization of the South Atlantic marine boundary layer aerosol using an
22 aerodyne aerosol mass spectrometer, *Atmos. Chem. Phys.*, 8, 4711–4728,
23 <https://doi.org/10.5194/acp-8-4711-2008>, 2008.

24

25

26

27

28

29

30

31

32

33

34

35

36

37

38

39

40

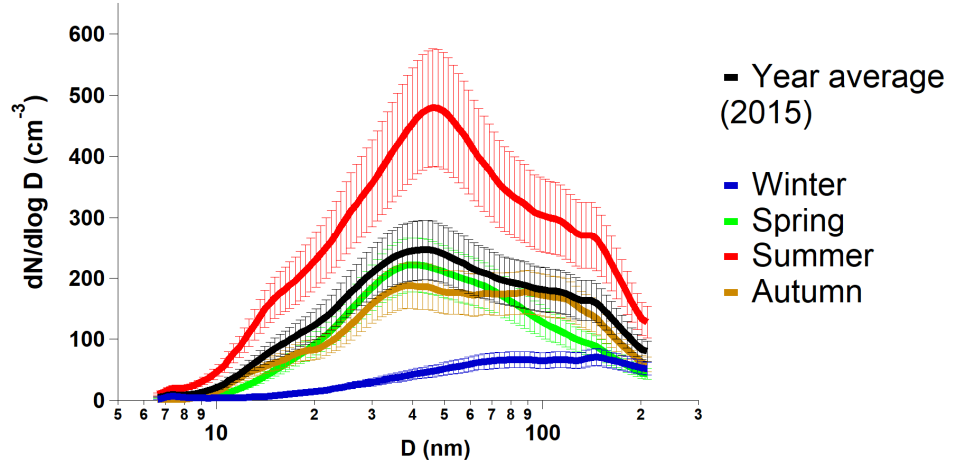
41

42

1
2
3
4
5
6
7
8

LIST OF FIGURES

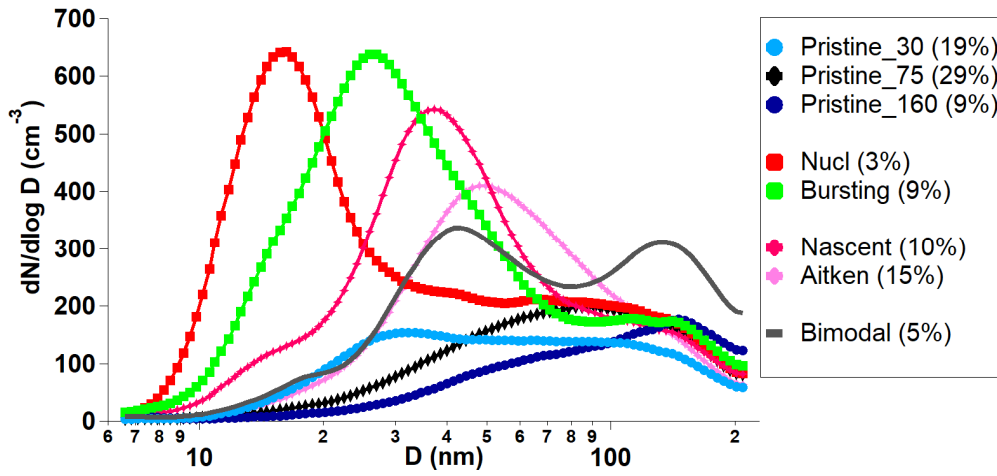
Eliminado: ¶
¶
¶
¶
¶
¶
¶
¶
¶
¶



9
10
11
12
13
14
15
16
17
18
19
20
21
22
23
24

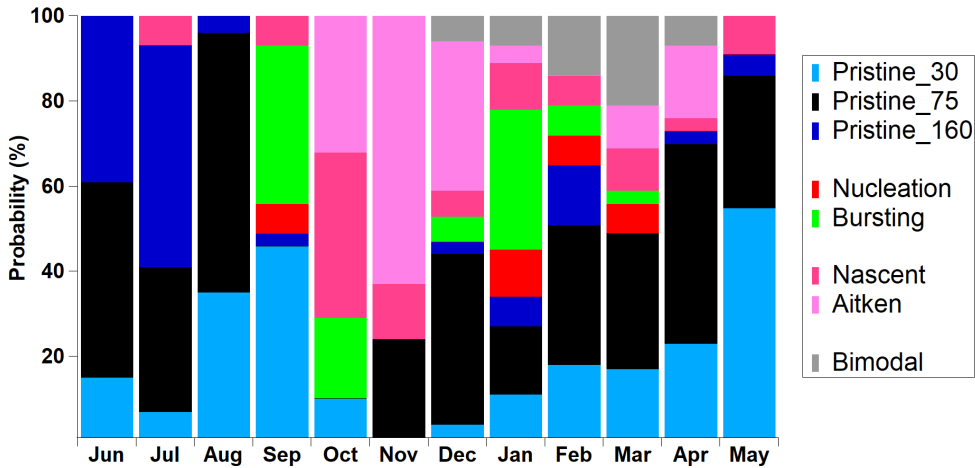
Figure 1 Seasonal mean aerosol size distribution measured by the SMPS at Halley VI research station over the year 2015. The error bars represent the standard deviation of the measurements from the mean value.

1
2



3
4
5
6

(a)



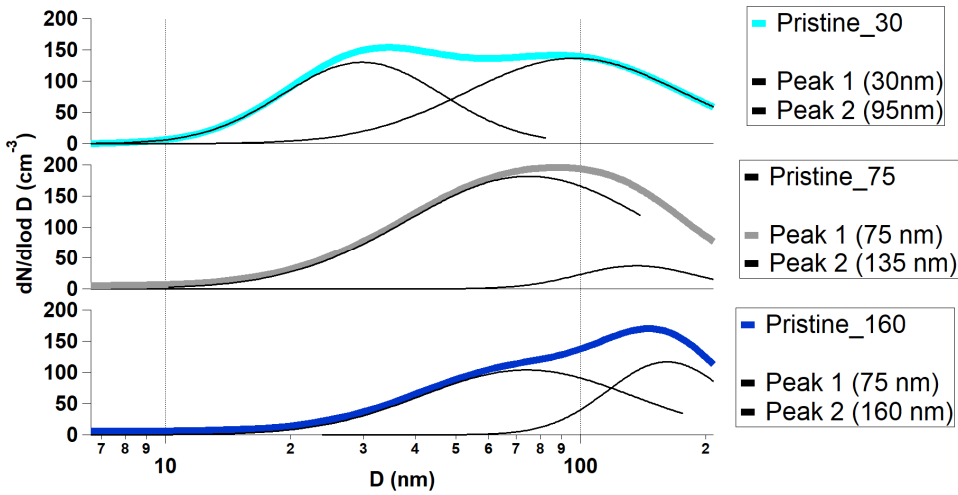
7
8
9

(b)

10 **Figure 2** (a) Size distributions of the 8 k-means clusters and (b) annual
11 frequency distributions of the six aerosol categories

12
13
14
15

1
2
3
4
5
6
7
8

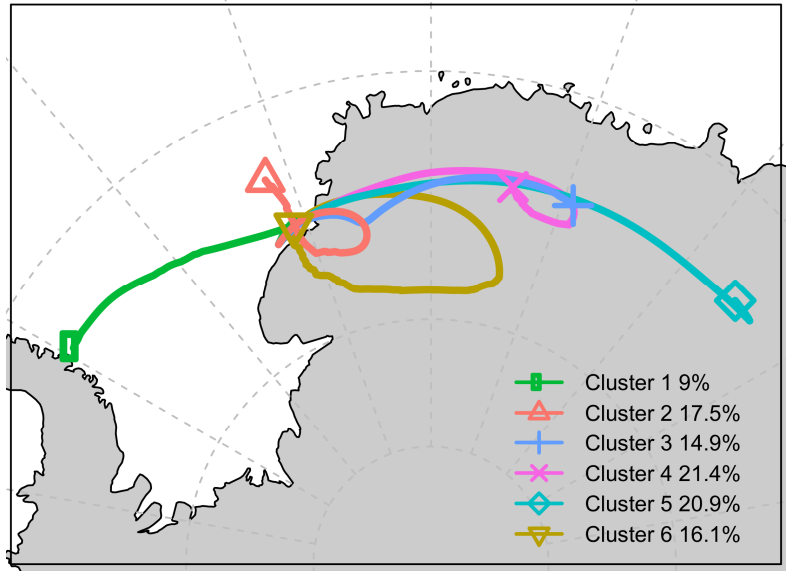


9

10 **Figure 3** Peak fitting of the 3 pristine K-means aerosol categories.

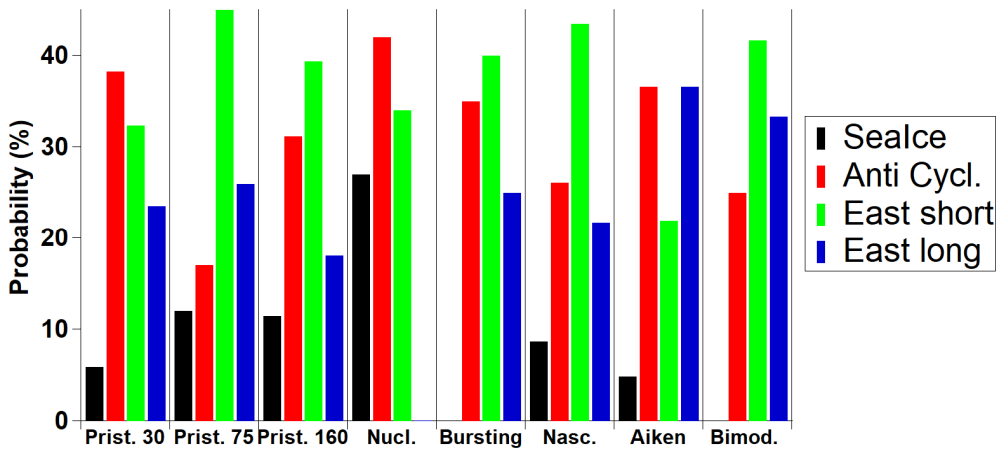
11
12
13
14
15
16
17
18
19
20
21
22
23
24

1
2
3



4
5

(a)



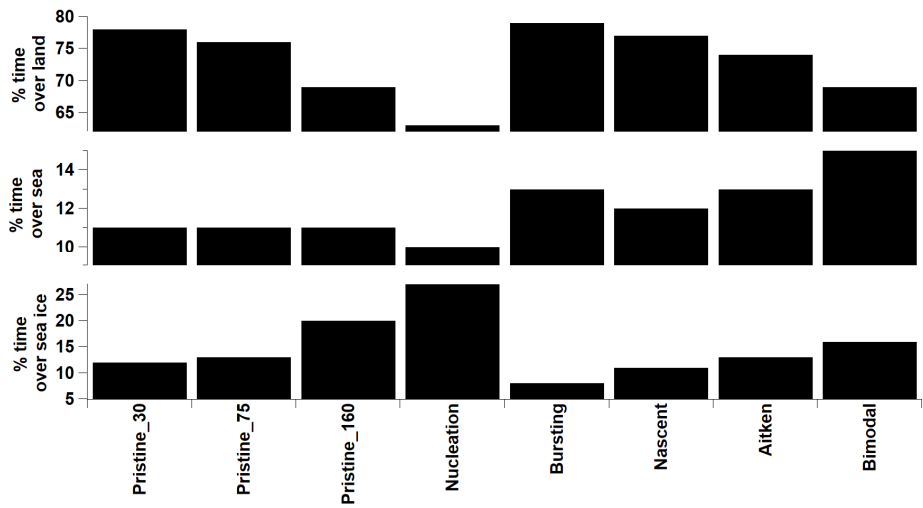
6
7

(b)

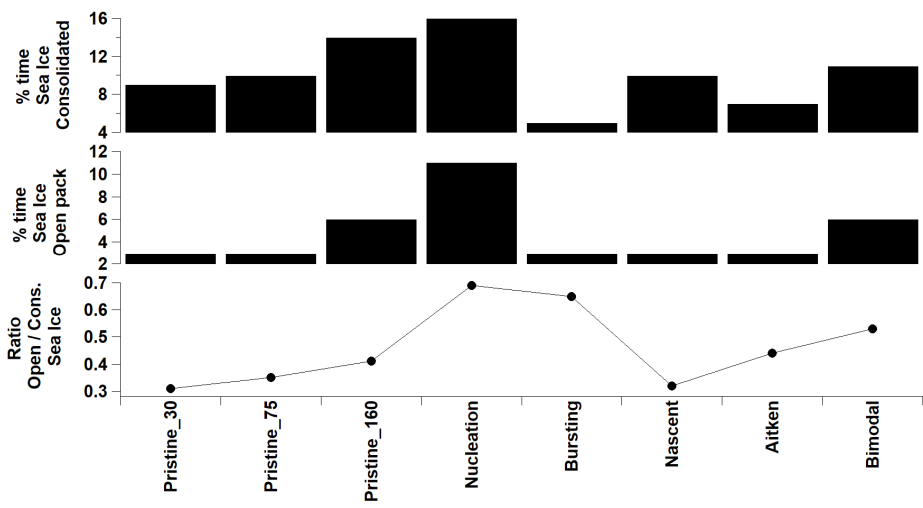
Figure 4 (a) Air mass analysis of air mass back trajectories arriving at Halley during the year 2015 (hourly resolution) and (b) relative contribution for each aerosol category. Groups in (b) are : Sea Ice (1), Anti Cycl. (2,6), East short (3,4) and east long (5),

Eliminado: 365

12
13
14



(a)



(b)

Figure 5 (a) Percentages of air masses over land, sea, and sea ice for the 8 K-means aerosol categories and (b) percentages of consolidated and open pack sea ice, and open pack / consolidated ratio.

1
2
3
4
5
6
7
8
9
10
11
12
13
14
15
16
17
18
19
20
21
22
23
24
25

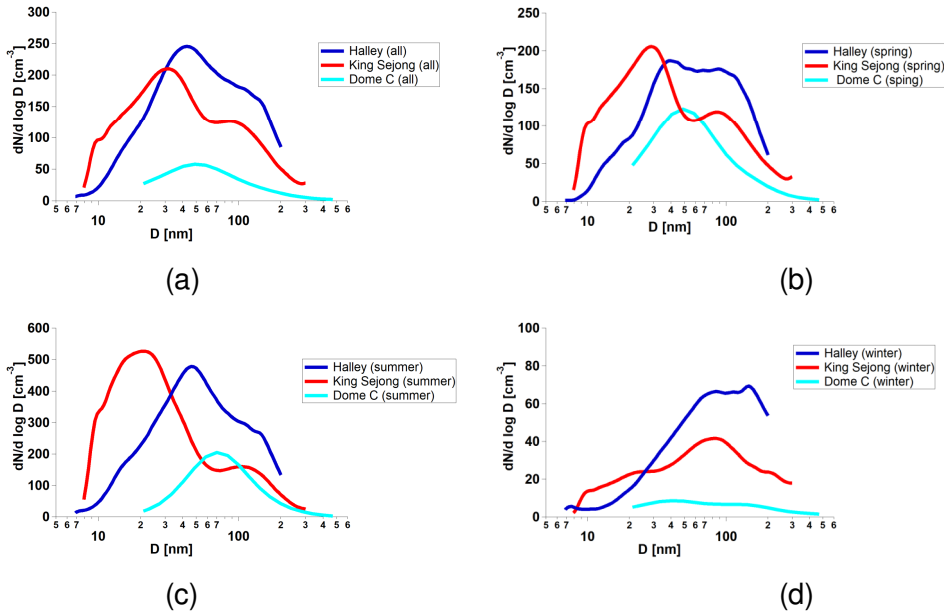
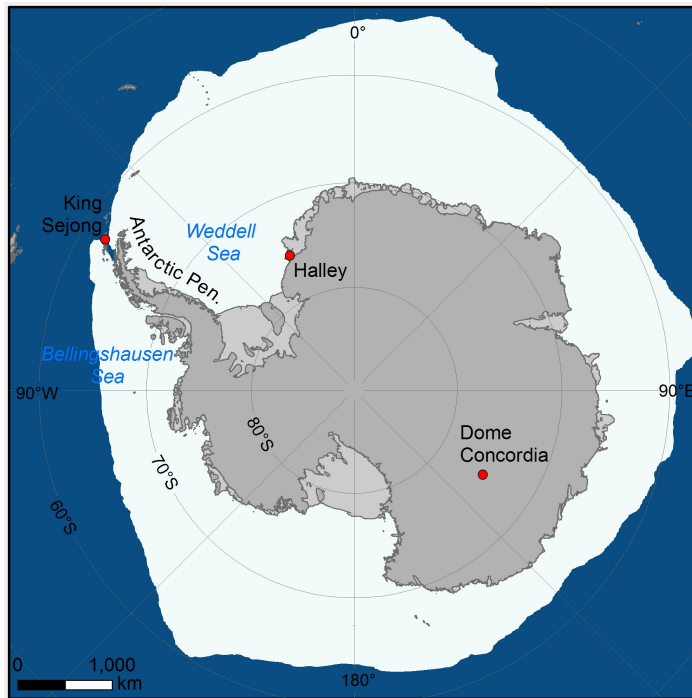


Figure 6. Average size-resolved particle size distributions simultaneously measured during the year 2015 at Halley, Dome C and King Sejong stations for (a) May-December (8 months), (b) spring (Sep., Oct., Nov., 3 months), (c) summer (December, 1 month) and (d) winter (Jun., Jul., Aug., 3 months).

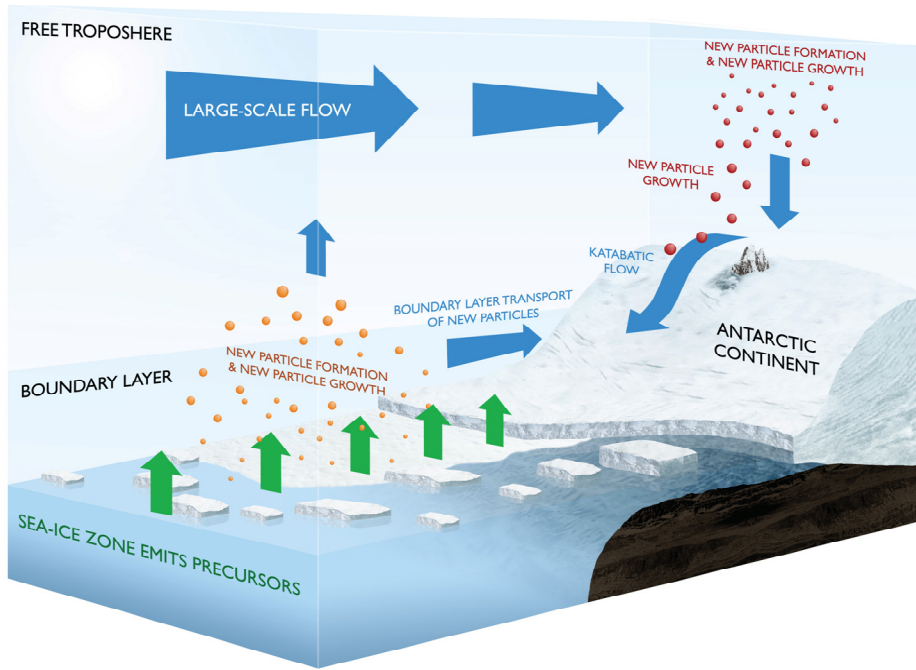
1
2



3
4
5
6
7
8
9
10
11
12
13
14
15
16
17
18
19
20

Figure 7. Map with locations of Antarctic monitoring stations considered in Figure 6. Please note that the sea ice extent is the median September extent from 1981-2010 (data are from NSIDC - <https://nsidc.org/data/g02135>).

1



2

3

4 **Figure 8** Schematic illustrations of the ultrafine New Particle Formation (NPF)
5 and New Particle Growth (NPG) aerosols in Antarctica.

6

7

8

9

10

11

12

13

14

15

16

17

18

Prior to clustering, the SMPS distributions are normalized so that the Euclidean length of each (treated as a vector) is 1. This ensures that we are clustering the shape of the distributions irrespective of the magnitude of the number count within each. The normalized data given then are clustered using the k-means (method R Core Team (2019)). This partitions the SMPS distributions (treated as vectors by k-means) into k groups such that the sum of squares of the distances from these points to the assigned cluster centres is minimized. At the minimum, the cluster centres form the average SMPS distributions of the individual SMPS distributions assigned to each cluster.

To decide on the number of factors to choose, the Dunn Index and Silhouette Width were calculated for each factor number. The Dunn Index is the ratio of the smallest distance between observations not in the same cluster to the largest intra-cluster distance. The Dunn Index has a value between zero and infinity, and should be maximized. Similarly, the Silhouette Width analysis is a measure of how similar the observations are with the cluster they are assigned to relative to other clusters. Its value ranges from -1 to 1 for each observation in your data. A value approaching 1 indicates that the elements within each cluster are identical to each other; a values close to 0 suggest that there is no clear division between clusters; and a value to -1 suggest that the observations have been assigned to the wrong cluster. As we increase the cluster number from 2 up to 30 the Silhouette Width falls from a maximum value of 0.49 to 0.28 and the Dunn Index increases from a minimum of 2.9×10^{-3} to a maximum 12.3×10^{-3} . As the number of clusters is increased from 2, the increase in Dunn Index reflects the sequential improvement of the fit as more clusters are offered to the algorithm to fit the various facets of the data. In comparison, the Silhouette Width decreases. Although the similarity of the elements within each cluster will increase, the dissimilarity between each cluster will decreases and this what drives the Silhouette Width down. When plotted an optimum of 8 clusters was decided upon (average Silhouette Width of 0.35 and a Dunn Index of 4.6×10^{-3}) based upon these two opposing factors. The first factor being the increase in the fit of the clusters to the

natural clusters within the data with increased cluster number and the second being the over clustering of the data such that the natural clusters are divided according to the natural spread of the points within the cluster. This can be determined by looking for so called 'knees' within the two plots.